The Dissertation Committee for Shariq Ali Certifies that this is the approved version of the following dissertation:

Paclitaxel nanoparticles for breast cancer therapy in pregnancy

Committee:

Erik Rytting, PhD (mentor)

Mahmoud S. Ahmed, PhD

Marxa Figueiredo, PhD

Sandra Hatch, MD

Jai S. Rudra, PhD

David Niesel, PhD

Dean, Graduate School

Paclitaxel Nanoparticles for Breast Cancer Therapy in Pregnancy

by

Shariq Ali, B.S.

Dissertation

Presented to the Faculty of the Graduate School of

The University of Texas Medical Branch

in Partial Fulfillment

of the Requirements

for the Degree of

Doctor of Philosophy

The University of Texas Medical Branch

May, 2017

Dedication

This dissertation is dedicated to my family and friends, who have supported me throughout my education.

Acknowledgements

First and foremost, I want to acknowledge and express my gratitude towards Dr. Erik Rytting. The work presented in this dissertation would not have been possible without his guidance and mentorship. I would also like to thank all of the past and present members of the Rytting lab, who have assisted in experiments, taught me many laboratory skills, and provided invaluable feedback regarding this project.

I also want to recognize the contributions of the Maternal-Fetal Pharmacology and Biodevelopment Laboratories at UTMB, many of whom were directly involved in the experimental design and execution, as well as data analysis. All of the members of this group have provided me with guidance and feedback that was critical to the progress of this project.

I would like to thank the members of this dissertation committee for providing me with suggestions for and critical analysis of the project. Their involvement and contributions have strengthened this project immeasurably.

The Department of Pharmacology and Toxicology and the Pharmacology and Toxicology Graduate Program at UTMB have helped me navigate the rigorous path of graduate school. For their input on this project and their guidance, I am grateful. I would also like to thank the School of Medicine for providing me with clinical knowledge and skills that have strengthened me as a scientist.

I would like to express my appreciation to the past and present members of the MD/PhD program for allowing me the opportunity and financial support necessary to receive my doctoral education at UTMB. The shared experiences and advice of students and faculty who comprise this program were essential for my progress as a student, and will continue to be throughout my doctoral education and beyond.

Finally, I would like to thank my family and friends for their continued support throughout this project. My parents, as well as my brother and his wife, have contributed essential guidance and perspective in my education.

The work presented here, as well the other projects that I have worked on at UTMB, were funded by the John Sealy Memorial Endowment Fund for Biomedical Research, the National Institutes of Health, Citizens United for Research in Epilepsy, and the Retina Research Foundation. I am thankful to be a part of the project supported by these organizations.

Paclitaxel Nanoparticles for Breast Cancer Therapy in Pregnancy

Publication No._____

Shariq Ali, Ph.D.

The University of Texas Medical Branch, 2017

Supervisor: Erik Rytting

Breast cancer can complicate pregnancy and result in fetal and maternal morbidity and mortality. These effects are often compounded by restrictions in the diagnosis and treatment of breast cancer due to implications on fetal health. A number of new paclitaxel nanoformulations for the treatment of breast cancer are entering clinical studies or are commercially available, but whether or not these formulations cause differences in transplacental transfer and, ultimately, fetal exposure remains to be seen. Here, we examined three formulations of paclitaxel—Taxol, or paclitaxel dissolved in Cremophor-EL; Abraxane, an albumin nanoparticle; and Genexol-PM, a polymeric micelle. Using the *ex vivo* dually perfused human placental cotyledon, we were able to show that paclitaxel transfer appears to be similar across the formulations, but the maternal concentrations and placental accumulation varies significantly. This is likely due to the interaction of the materials with the placental trophoblast, so we also examined the formulations in a trophoblast cell model for their susceptibility to efflux, as well as the permeability and uptake of fluorescent nanoparticle analogues. We found that Genexol-PM allows paclitaxel to overcome P-gp efflux and crosses the trophoblast to a significant extent, while Abraxane behaves like a free drug formulation. Cremophor-EL in Taxol is believed to cause differences in paclitaxel permeability across the apical trophoblast membrane as

well. We anticipate that these findings will have an impact on the future design of pharmaceuticals tailored to pregnancy-related diseases, but also in the development of rational and safe treatment strategies for pregnancy-associated breast cancer and other diseases.

TABLE OF CONTENTS

List of Tables

List of Figures

List of Abbreviations

7-MC	7-methoxycoumarin-3-carbonyl azide
ACN	Acetonitrile
ATP	Adenosine triphosphate
CT	Computed tomography
DMEM	Dulbecco's modified Eagle's medium
DMF	Dimethylformamide
DMSO	Dimethyl sulfoxide
ER	Estrogen receptor
fHSA	Fluorescein-labeled human serum albumin
gp60	Albondin
HBSS	Hank's balanced salt solution
HER2/neu	Human epidermal growth factor receptor 2
HPLC	High performance liquid chromatography
HPPS	High performance particle sizer
HSA	Human serum albumin
MDR1	Multidrug resistance protein 1 (P-glycoprotein)
mPEG	Methoxypolyethylene glycol
MTD	Maximum tolerated dose
NHS	N-hydroxysuccinimide
PDA	Photodiode array detector
PDLLA	Poly(D,L)lactic acid
PET	Positron emission tomography
P-gp	P-glycoprotein (multidrug resistance protein 1)
PR	Progesterone receptor
SPARC	Secreted protein acidic and rich in cysteine (osteonectin)
TEER	Transepithelial electrical resistance
THF	Tetrahydrofuran
UV	Ultraviolet

Chapter 1. Introduction

There are many challenges in the treatment of diseases that occur during pregnancy. Diagnostic imaging and administration of pharmaceuticals during pregnancy in particular must be conducted carefully to avoid undue harm to the mother or fetus. Of these diseases, the diagnosis and treatment of breast cancer during pregnancy is one of the most dire due to the associated high mortality, as well as the harmful effects of chemotherapy and radiotherapy on the fetus. This project was designed to address some of the concerns associated with treating this disease.

This dissertation is divided into four chapters. The first chapter is an introduction to the topic and an evaluation of the current status of breast cancer therapy during pregnancy. We examine the complications associated with typical diagnostic and treatment protocols when breast cancer occurs during pregnancy. This is followed by a discussion of the drug paclitaxel, which is used in breast cancer therapy and is the focus of this project. Chapter two is an examination of the transplacental transfer of three formulations of paclitaxel that are used in pregnancy using the *ex vivo* dually perfused human placental cotyledon model. These formulations are Taxol® (paclitaxel dissolved in Cremophor®-EL), Abraxane® (a paclitaxel-loaded albumin nanoparticle), and Genexol®-PM (a paclitaxel-loaded polymeric micelle, also known as Paxus®-PM or Cynviloq®). Chapter three then focuses on the mechanisms by which these three different types of formulations affect the transplacental transfer of paclitaxel. In particular, mechanisms of efflux and endocytosis are probed using pharmacological inhibitors in order to understand the findings of chapter two, as well to gain a better understanding of drug formulations and drug-loaded nanoparticles as a whole as they relate to pregnancy. Finally, chapter 4 is a summary of the findings and a conclusion of the dissertation.

BREAST CANCER IN PREGNANCY

Cancer as a whole has an occurrence of 1 in 1000 pregnancies (1). The most common types of cancer that occur in pregnancy are malignant melanoma, cervical cancer, lymphoma, and breast cancer (2). Of the types of cancers that occur in pregnancy, breast cancer is one of the most common, presenting in approximately 1 of every 3000 pregnancies (1,3). It is also the most common cause of cancer-related death in women who are pregnant or lactating (4). Generally, it is agreed that the incidence of breast cancer in pregnancy is rising. The explanation is that age is a risk factor, and there is an increasing trend for women to choose to become pregnant later in life (5). In addition to this, there exist many additional challenges in the diagnosis and treatment of breast cancer in pregnancy. At the present, there is a critical need to address this disease from the aspects of both improved treatment options and diagnostic procedures.

Challenges in diagnosis

Challenges in the diagnosis of this disease in pregnancy stem from physiological changes that can mask the symptoms of breast cancer and safety concerns associated with diagnostic procedures. Generally, breast tissue tends to proliferate during pregnancy, causing enlargement and changes in breast density. Though these changes occur normally, they can often mask tumor growth or other changes that occur with breast cancer (4). Estimates of the delay in diagnosis that occurs as a result of these changes range from 1 to 10 months. Delays can occur even after pregnancy, as physiological changes in breast tissue do not revert to normal until 1 to 5 months post-lactation (3,4). An additional feature of pregnancy-associated breast cancer is that these cases are 2 to 2.5 times more likely to have metastatic disease than in non-pregnant patients. Lymph node involvement is more common and tumor sizes are generally larger. One explanation for this is that the delay in

diagnosis allows this to happen, but it is still unclear if there are any underlying differences in the aggressiveness of breast cancer between pregnant and non-pregnant patients (3).

Further challenges in diagnosis occur in radiological procedures that are either not as sensitive or contraindicated in pregnancy. Mammography is one of the most common radiological diagnostic tools that is used, and has the advantage of being able to visualize malignant calcifications. This procedure involves the use of ionizing radiation, but can be conducted safely with appropriate abdominal shielding. There is some evidence that mammography has reduced sensitivity (higher false negative rate) in pregnancy, although different reports reach different conclusions regarding this matter (3,6). Regardless of this, other radiological procedures may be used to support the diagnosis. Computed tomography (CT) is strictly contraindicated in pregnancy due to the substantially larger ionizing radiation dose given compared to chest x-ray or mammography (4). Though magnetic resonance imaging is permitted in pregnancy, gadolinium contrast is not allowed due to its ability to penetrate the placenta and the unknown effects on fetal health (4,7,8). Positron emission tomography (PET) scans and bone scans are also to be avoided during pregnancy because they necessarily require the use of positron emission, which is a type of potentially harmful radiation (8). Ultrasound has been shown to be substantially more sensitive than mammography, and is safe to use in pregnancy (6). Additionally, solid tumors and non-solid tumors can be differentiated by the use of ultrasound (4).

Challenges in treatment

There are a number of challenges associated with breast cancer treatment in pregnancy. These are most often associated with the harmful effects of available treatment options to the fetus. Cytotoxic chemotherapy is a major component of most cancer therapy regimens. However, the decision to use chemotherapy in these patients must be weighed carefully. Depending on the type of drug to be used, the time of gestation during which it

is administered, and the dose, chemotherapy can cause severe fetal toxicity, teratogenicity, and even fetal mortality (7,8). Depending on the extent of disease and receptor status, typical treatment regimens may include some form of surgical incision, breast conserving therapy, or mastectomy.

Most cases of breast cancer in pregnancy demonstrate low expression of estrogen and progesterone receptors (ER and PR), but they have higher expression of human epidermal growth factor receptor 2 (HER2/neu) (3,4,7). The impact that these features have on the aggressiveness of the cancer is complex, because different hormones can have different effects on tumor cell proliferation. However, treatments that target these hormone receptors are contraindicated in pregnancy due to their side effects. One example of this is trastuzumab, which is a monoclonal antibody designed to target HER2/neu. It is known in pregnancy that administration of this drug causes oligohydramnios, probably due to fetal renal failure (7,9,10). Maternal hormone levels are also quite important during pregnancy, especially estrogen levels, for the developing fetus. Tamoxifen, an estrogen receptor blocker, is also contraindicated in pregnancy due to teratogenic effects and fetal mortality (3,9).

Current treatment strategies for breast cancer in pregnancy

According to the National Comprehensive Cancer Network Guidelines, the treatment for breast cancer in pregnancy can include surgery and chemotherapy. Initial surgical treatment of breast cancer presenting in pregnancy should proceed in a similar manner to the typical treatment in non-pregnant patients. These include breast-conserving surgery or mastectomy, and can be done safely during pregnancy. Breast-conserving therapy may require adjuvant radiotherapy, and therefore may be more feasible if adjuvant radiotherapy can be delayed until after delivery. This is because radiotherapy is strictly contraindicated at every stage in pregnancy (7,8).

The NCCN guidelines state that chemotherapy regimens for invasive breast cancer in non-pregnant patients can include anthracyclines (doxorubicin or epirubicin), 5-fluorouracil, cyclophosphamide, and taxanes (paclitaxel or docetaxel). Generally, these regimens include combinations of anthracyclines with cyclophosphamide and 5-fluorouracil, and are followed by the administration of taxanes. In some instances, these regimens can include anti-HER2/neu, depending on the receptor status of the patient. Hormone therapy regimens may include tamoxifen and aromatase inhibitors. However, as mentioned before, no hormone therapy or anti-HER2/neu antibodies may be used during pregnancy, and thus the treatment options are limited to the aforementioned cytotoxic compounds (7,8). These are generally considered safe in pregnancy, provided they are administered at the correct point in gestation. It is typically recommended that preoperative and postoperative chemotherapy be administered in the second and early third trimesters. During the first trimester, the risk of teratogenicity is too high to allow for chemotherapy use (7). Later in the third trimester, around 34 weeks gestation or a few weeks prior to scheduled delivery, chemotherapy is stopped to avoid hematological complications (7,8).

Taxanes, and paclitaxel in particular, are a mainstay of most treatment regimens for breast cancer during pregnancy. Even though examples of teratogenicity caused by first trimester exposure to chemotherapeutics can be found in the literature, little is known about the direct effect of taxanes on human fetal development. Teratogenicity has been shown to occur in animal models with exposure to taxanes during organogenesis (9,11,12), but there are few reported cases where taxanes themselves are administered during the early periods of pregnancy. Generally, taxanes are seen as safe during pregnancy (7,8,13). Their transplacental transfer in term placentas (using the *ex vivo* dually perfused human placental cotyledon model, discussed in detail in the next chapter) has also been shown to be fairly low (14,15). An important note regarding the reported outcomes of pregnancies in which paclitaxel was administered is that long term outcomes of these pregnancies have yet to be thoroughly investigated (7,13).

PACLITAXEL

As mentioned before, paclitaxel belongs to a group of compounds known as taxanes. Paclitaxel weighs 853.9 g/mol and has a calculated octanol/water partition coefficient (logP) of 4.0 (16). It was originally isolated from the tree *Taxus brevifolia*, though since then a number of procedures for the total synthesis of paclitaxel have been established (17). Taxanes are generally cytotoxic, and exert their effects through microtubule binding. Microtubules are subcellular filaments that are involved in a variety of cellular processes, including trafficking and cell division, and function by the polymerization and depolymerization of α- and β-tubulin dimers (18). By binding to the β-tubulin subunit of microtubules, they prevent their depolymerization, effectively preventing cell division and halting the cell cycle in the G2/M phase (Figure 1.1). There may be other mechanisms involved in the mechanism of toxicity of paclitaxel, including interactions with the cell during interphase. The reason this has been suggested is that the mitotic rate of most tumors has been calculated to be too slow to allow for the rate of tumor shrinkage caused by paclitaxel (19).

Paclitaxel is used to treat multiple types of malignancies, which include breast cancer, ovarian cancer, lung cancer, and Kaposi's sarcoma. Typically, paclitaxel is available as Taxol, which is paclitaxel dissolved in Cremophor-EL. Before alternative formulations were developed, the use of a co-solvent was necessary because paclitaxel has very poor water solubility. Cremophor-EL is made of polyethoxylated castor oil and dehydrated ethanol, and the formulation Taxol is actually prepared for administration by dilution of Taxol into saline (20). Taxol is associated with a number of adverse effects, which may be due to either paclitaxel or Cremophor-EL. Side effects of Cremophor-EL largely include acute hypersensitivity reactions, including difficulty breathing, rash, edema, hypotension and tachycardia. Because of these reactions, patients are often pre-medicated with anti-inflammatory drugs such as corticosteroids and histamine receptor

blockers, though some of these effects are still seen in a large percentage of patients (21). Because of these effects, there has more recently been a surge of alternative formulations of paclitaxel that allow for suspension of the drug in saline for injection while avoiding the administration of Cremophor-EL. Some of these formulations have been approved for use in patients in the US, while others are in clinical development (Table 1.1).

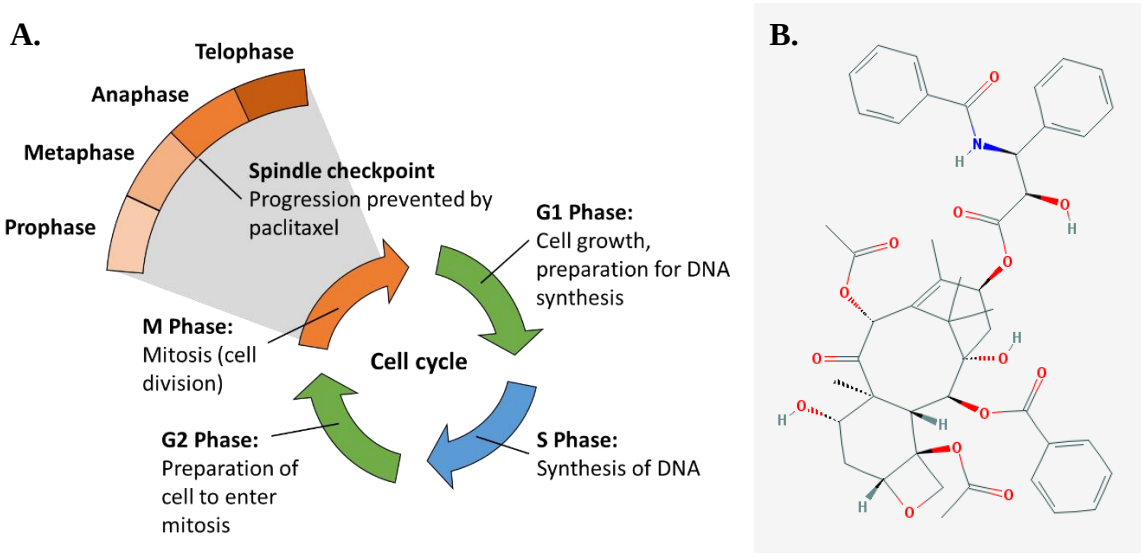

Figure 1.1. Mechanism and structure of paclitaxel.

(A) Typically, the cell cycle is represented as four distinct phases. Paclitaxel prevents progression through mitosis by stopping the cell at the spindle checkpoint (19,22). (B) Structure of paclitaxel, taken from PubChem Open Chemistry Database <https://pubchem.ncbi.nlm.nih.gov>.

Paclitaxel is metabolized largely by hydroxylation to form 6α-hydroxypaclitaxel, by CYP2C8, and 3'-hydroxypaclitaxel, by CYP3A4 (23). To our knowledge, paclitaxel metabolism by the placenta is most likely negligible; CYP2C8 expression has been shown in the placenta at the mRNA level at very low concentrations and may be involved the

metabolism of buprenorphine to a limited extent (24–26). CYP3A4 has likewise been shown at the mRNA level (27). However, as of now there is no evidence that paclitaxel is metabolized by the placenta. Esters that are present within paclitaxel may also subject to pH-dependent hydrolysis (Figure 1.1B) (28).

Table 1.1. Examples of paclitaxel formulations

Formulation name	Description	Clinical development phase	Sources
Taxol	Paclitaxel dissolved in Cremophor-EL	Approved in US	(29,30)
Abraxane (nab-paclitaxel, ABI-007)	Albumin nanoparticle (130 nm), made of human serum albumin	Approved in US	(29–32)
Genexol-PM (Paxus-PM, Cynviloq, IG-001)	Polymeric micelle (23 nm), made with methoxy-poly(ethylene glycol)-b-poly(D,L)lactide	Approved in South Korea; Phase II in US	(20,29,33)
Paclical (Apealea)	Micelle (20-60 nm), based on the XR-17 platform, derived from Vitamin A	Approved in Russia; Phase III in US	(29,34)
Lipusu	Liposome (400 nm), composed of cholesterol and lecithin	Approved in China	(29,35,36)
Paclitaxel injection concentrate for nanodispersion (PICN, SPARC1507)	Nanoparticle (100-150 nm), made with polyvinylpyrrolidone, octanoic acid, and cholesterol sulfate	Approved in India; Phase III in US	(29,37)

Examples of paclitaxel nanoformulations in various stages of clinical development are shown here. Alternative designations of nanoformulations are given in parentheses next to the name. Clinical trial information is available at <https://clinicaltrials.gov>.

NANOPARTICLES AS DRUG FORMULATIONS

Having an effective and convenient delivery method for pharmaceuticals is arguably one of the most important aspects of drug and formulation development. In the case of Taxol, poor water solubility led to the administration of paclitaxel dissolved in Cremophor-EL. Because of the risks of hypersensitivity reactions that are caused by Cremophor-EL, many new formulations of paclitaxel, mostly using nanoparticles, have emerged (38,39). Nanoparticles typically measure tens to hundreds of nanometers in diameter, but are smaller than one micron. They may vary in their stability, surface charge, the material from which they are made, and their biocompatibility. Nanomaterials have a number of applications, including many biomedical applications such as for imaging and drug delivery applications (40–42). In the context of drug delivery, such as formulations of paclitaxel, nanoparticles are designed from biocompatible (in some cases, biodegradable) materials that hold drug molecules either through degradable covalent bonds or through lipophilic or ionic interactions between the drug and the material (20,40,43).

Though the use of nanomaterials is not necessary for administration of drugs, it does possess a number of advantages. One of the potential advantages is that nanoparticles may improve the solubility of a compound in aqueous media. One of the key advantages of Abraxane®, a nanoparticle made of human serum albumin and loaded with paclitaxel, is that paclitaxel was effectively able to be suspended in aqueous media, i.e. saline, without the need for Cremophor-EL (38,39). Another advantage of some nanoparticles is that, depending on the material from which it is made, they may allow for controlled and sustained release of a compound into the bloodstream. Compounds that may have unfavorable pharmacokinetics or that require relatively high dosing intervals may benefit from being administered this way (44).

One of the most important and exploited advantages of nanoparticles is their ability to deliver a drug to certain parts of the body while avoiding others. Nanoparticles may accumulate in tumors, for example, due to their diameter and the porous nature of the endothelium of solid tumors, which is notoriously leaky (45). Depending on the type of nanoparticle, penetration of biological barriers may be limited or enhanced. As an example, it has been shown that poly(amidoamine) dendrimers have very little placental penetration, while other polymeric nanoparticles such as polystyrene or PEGylated poly(lactide-co-glycolide) may have much more penetration (46,47). Further, it was shown that encapsulation of digoxin in polymeric nanoparticles may allow digoxin to cross the placental efflux barrier *in vitro* when compared to free digoxin (48). Active targeting of nanoparticles to specific tissues can also be achieved by conjugating the surface of nanoparticles to ligands that can bind with cell surface receptors. This may induce receptor mediated endocytosis and can lead to increased accumulation in a specific tissue (49).

PROJECT OVERVIEW

Patients and physicians are confronted with very difficult decisions when determining how best to treat breast cancer during pregnancy. As it stands, there is a very limited amount of data regarding diagnostic and treatment strategies, in particular the safety of these methods and their impact on fetal health. Deciding whether or not it's best to wait until after delivery to begin treatment, what diagnostic tests to use, and what treatment strategies are most likely to preserve the health of the fetus and the mother are just some of the choices that need to be made. Paclitaxel is likely to be part of many treatment regimens due to its safety (during certain phases of pregnancy) and efficacy. Because administration of nanoparticle formulations of paclitaxel may reduce the risk of hypersensitivity reactions, they may be preferable to administer. However, it is well known that encapsulation in nanoparticles may, in some cases, enhance the permeability of a drug

across a biological barrier. On the other hand, it is possible that some materials limit the extent of transplacental transfer of compounds across the placenta, potentially making them safer to use during pregnancy. There is currently little or no data regarding the impact of nanoformulations on transplacental drug transfer.

We designed this project to determine the extent to which different nanoformulations affect the transplacental transfer of paclitaxel, using both an *ex vivo* model of term human placentas, as well as an *in vitro* cell culture model. The first two nanoparticle formulations we chose are Abraxane, which is approved for clinical use, and Genexol-PM, which is currently under trials for bioequivalency to Abraxane in the United States. The results of this project will shed some light on the role that nanoformulations of paclitaxel may play in the treatment of pregnancy-associated breast cancer. We also anticipate that the knowledge gleaned from these experiments may guide future hypotheses and projects investigating the potential role of nanoparticles in treating other pregnancy-related illnesses.

Chapter 2. Transplacental transfer of clinically available paclitaxel formulations

INTRODUCTION

A number of formulations of paclitaxel have been investigated in clinical trials, and some are also entering the market (Table 1.1). The concerns with using these formulations in pregnancy stem from their potential ability to increase fetal exposure to paclitaxel, thus increasing the risk for fetal morbidity and mortality. Two of these formulations are Genexol-PM and Abraxane, which were developed to improve the solubility of paclitaxel and prevent the need to use Cremophor-EL as a co-solvent. Though this is potentially useful in preventing the need for premedication with anti-inflammatory steroids, the ability of these materials to influence the transport of paclitaxel across the placenta is largely unknown.

Abraxane is a nanoparticle that is prepared from human serum albumin (Figure 2.1). This formulation takes advantage of the high protein binding of paclitaxel. Abraxane is prepared by forming an emulsion of albumin nanoparticles by high pressure homogenization with an organic solvent containing paclitaxel. The organic solvent is then removed by evaporation and the suspension is sterile filtered and lyophilized (50). The resulting nanoparticles, which are approximately 130 nm in diameter and contain no cross-linkers, are easily dispersed in saline, bypassing the need for Cremophor-EL (38). This results in a higher maximum tolerated dose (MTD) of 300 mg/m^2, compared to Taxol which has an MTD of 260 mg/m^2 (29). However, the ability of these nanoparticles to cross the placenta is not known. One key feature of Abraxane is that it disintegrates upon dilution into plasma. Because of this, it is often characterized as an immediate release formulation, because upon disintegration, Abraxane becomes a solution of albumin-bound paclitaxel (51). It has been shown that albumin in maternal circulation has the ability to enter the

human placental trophoblast in placental explants, likely through a clathrin-dependent process. Little to no albumin transfer to the fetal circulation was seen; rather, albumin was recycled into the maternal circulation (52). The reasons for this process occurring are unknown; however, they may have an impact on Abraxane transport across the placenta, and specifically albumin-bound paclitaxel, if it undergoes a similar process. It's also known that protein binding typically limits the transplacental transfer of drugs, as has been shown in perfusions of paclitaxel comparing 2 and 30 mg/mL human serum albumin in perfusion medium (15) as well as anti-nicotine antibodies preventing the transfer of nicotine across the placenta (53). The extent to which this translates to nanoparticles made of protein is not known.

Unlike Abraxane, Genexol-PM is prepared from a synthetic block co-polymer (Figure 2.1). This polymer consists of poly-(D,L) lactic acid (PDLLA, 1750 Da), which is a polyester that hydrolyzes to lactic acid, and polyethylene glycol (PEG, 2000 Da), which has been shown to be biocompatible but is not biodegradable. The PEG is capped on one end by a methoxy group. This formulation is prepared by dissolving both the polymer and paclitaxel in an organic solvent and then dispersing them in water, yielding micelles. Organic solvent is removed and the suspension is sterile-filtered and lyophilized (54). This formulation also does not require the use of Cremophor-EL as a co-solvent. Interestingly, this formulation is also considered an immediate release formulation, and has even entered bioequivalence clinical trials with Abraxane for metastatic breast cancer treatment. Information provided by the makers of Genexol-PM have shown that the micelles disintegrate in the bloodstream in a similar manner to Abraxane. They also exhibit similar pharmacokinetics to Abraxane, including a C_{max} of approximately 20 μg/mL (55). Genexol-PM also boasts a high MTD of greater than 300 mg/m^2, which is similar to Abraxane (29). Though little is known regarding the transport of albumin nanoparticles across the placenta, significantly more is known about the transport of synthetic polymeric nanoparticles across the placenta. Polymeric nanoparticle transport across the placenta is

size dependent, where smaller particles are more likely than larger nanoparticles to traverse the trophoblast and enter fetal circulation. This was shown using polystyrene nanoparticles in placental perfusions (model described in detail below), as well as PEGylated poly(lactide-co-glycolide) nanoparticles in BeWo cells, which are a choriocarcinoma cell line that is used as a model for the placental trophoblast (47,56). In addition, it has been shown that encapsulation of drugs within polymeric nanoparticles may prevent their efflux (48).

This chapter examines the transplacental transport of paclitaxel in these formulations. The placenta is an organ that develops during pregnancy, and has many roles in maintaining pregnancy and fetal health, including endocrine activity and nutrient transport. It also acts as a barrier, reducing the transfer of xenobiotics that may be present in maternal circulation into the fetal compartment (57,58). The placenta is structured so that between the maternal and fetal circulations there lie both the placental trophoblast cells (an epithelial cell barrier) as well as an endothelium lining the fetal capillaries. The capillaries branch out from arteries and veins from the umbilical cord into villous trees, which are surrounded by the trophoblast layer, outside of which flows maternal blood (Figure 2.2).

Much of the function of the placenta in terms of both nutrient transport and limited transfer of xenobiotics is due to the presence of both active (ATP-driven) and passive transporters that selectively take up solutes from the maternal circulation or efflux solutes out to the maternal circulation. As an example, the family of multidrug resistance proteins is able to use energy derived from ATP to efflux molecules from within the cell to the outside. MDR1 is also known as P-glycoprotein (P-gp), a member of the multidrug resistance protein family. It is positioned on the apical membrane of the trophoblast cell layer and can efflux molecules from the trophoblast cells back into the maternal circulation (59–61).

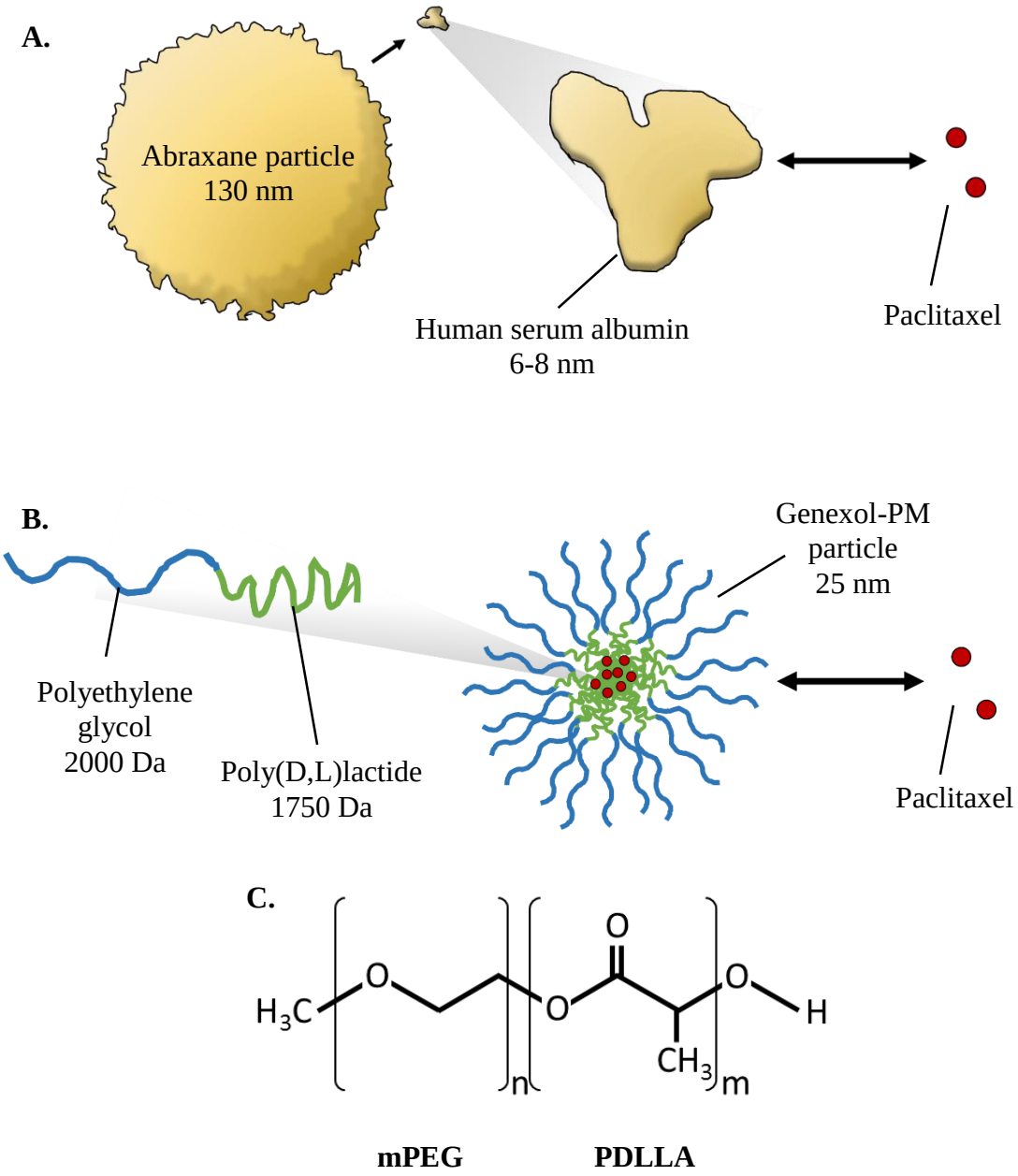

Figure 2.1 Visual representations of Abraxane and Genexol-PM

(A) Abraxane is an albumin nanoparticle formulation of paclitaxel. Human serum albumin (hydrodynamic diameter approximately 7 nm) is able to dissociate from the particle. On average, 8-9 paclitaxel molecules are loaded on each molecule of albumin in Abraxane (drug loading approximately 10%) (38,62,63). (B) Genexol-PM is a polymeric micelle made of a hydrophobic segment, poly(D,L)lactide, and a hydrophilic segment, polyethylene glycol. The polymer self-assembles into a micelle 25 nm in diameter, with paclitaxel in the hydrophobic core (drug loading approximately 10%). (C) Structure of mPEG-PDLLA used in Genexol-PM, with *n* molecules of ethylene glycol and *m* molecules of lactic acid.

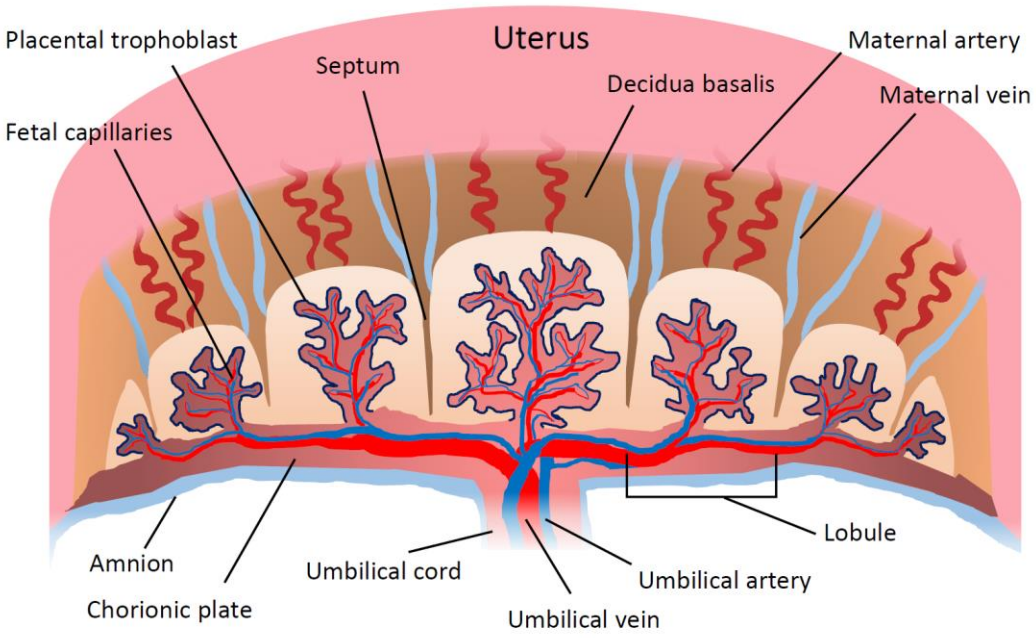

Figure 2.2 Anatomy of the human placenta

The human placenta is a transient organ that has many functions during gestation. It develops inside the uterus, and selectively allows passage of nutrients and other substances between the fetal and maternal circulations.

Transport across and uptake into the placenta was evaluated by the dually perfused human placental cotyledon model. In this model, term human placentas from uncomplicated pregnancies are catheterized in a single lobule and perfused with medium (Figure 2.3). Pharmaceuticals and xenobiotics can be added in the maternal or fetal circulation, and samples of perfusion medium can be taken to determine the transfer or accumulation of those products (14).

We hypothesized that the transport of paclitaxel across the placenta when formulated as Abraxane would be limited when compared to Taxol. If albumin nanoparticles are similarly taken up and recycled in the maternal circulation, any nanoparticle-bound paclitaxel may be ejected with the nanoparticle. In addition, dissociated paclitaxel would be subject to P-gp efflux. Taxol contains Cremophor-EL,

which has been shown in some instances to be an inhibitor of P-gp. However, the difference in size between Abraxane and albumin may influence the ability of the protein and paclitaxel to enter the trophoblast, and it is unknown what effect size has on the proposed mechanism of clathrin-mediated recycling of albumin. Further, we hypothesized that encapsulation of paclitaxel in Genexol-PM would enhance permeability across the placenta and increase accumulation in the tissue. Synthetic polymeric nanoparticles, including PEGylated biodegradable polyester nanoparticles, have been shown to be able to cross the placental membrane, and they have also been shown to shield P-gp substrates from P-gp efflux. This hypothesis was tested by comparing maternal, fetal, and placental concentrations of paclitaxel in the placental perfusion model using the three formulations.

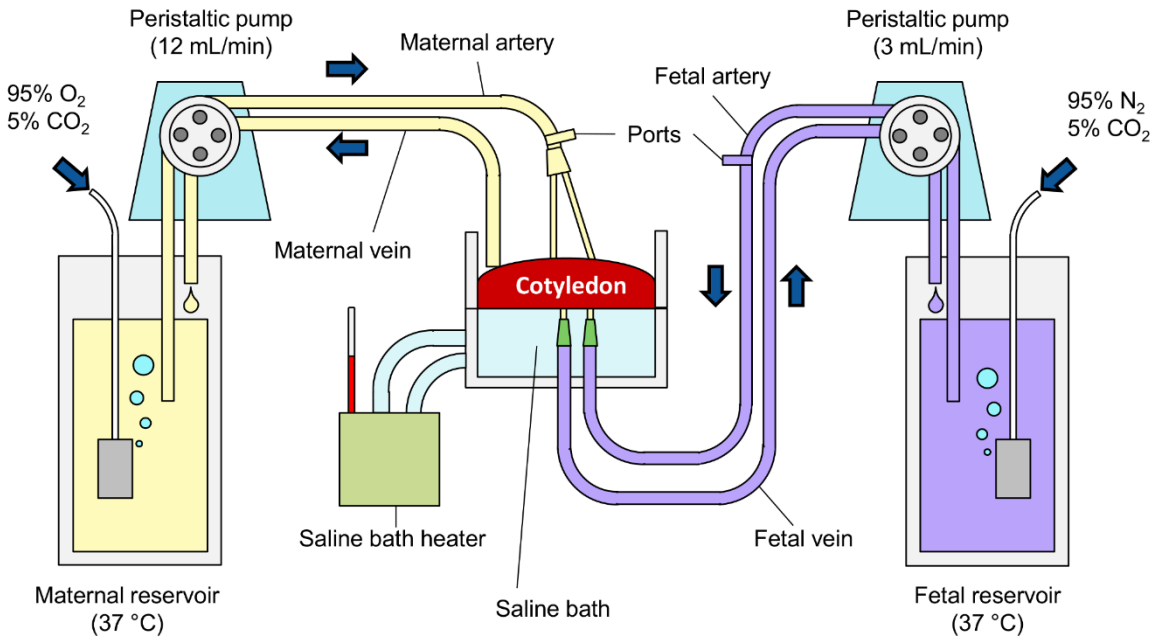

Figure 2.3 Placental perfusion apparatus

Human placentas are catheterized on the fetal and maternal sides, and perfused with M199 perfusion medium containing 30 mg/mL albumin. Samples can be taken from both reservoirs, as well as the maternal artery and fetal vein, for the duration of the experiment.

MATERIALS AND METHODS

Materials

Paclitaxel and celecoxib were obtained from TSZ Scientific LLC (Framingham, Massachusetts). Antipyrine, heparin sodium salt, gentamicin sulfate salt, dextran, and medium 199 with Earle's Salts were obtained from Sigma Aldrich (St. Louis, Missouri). Trimethoprim/sulfamethoxazole was obtained from SICOR pharmaceuticals, Inc. (Irvine, California). Normal saline (0.9% sodium chloride in water) was obtained from Nurse Assist, Inc. (Fort Worth, Texas). Chloroform (HPLC grade), acetonitrile (HPLC grade), sodium bicarbonate, and formic acid were obtained from Fisher Scientific (Waltham, Massachusetts). Human serum albumin was obtained from Calbiochem (La Jolla, California). Semisynthetic paclitaxel injection in Cremophor-EL (Taxol equivalent) was obtained from Mylan (Canonsburg, Pennsylvania). Abraxane was obtained from Abraxis BioScience (Los Angeles, California). Paxus-PM (Genexol-PM equivalent) was obtained from Kalbe International (Singapore).

Placental perfusion

Placental perfusion medium was prepared by dissolving M199 medium with Earle's salts (11 mg/mL), gentamicin sulfate (33.3 μg/mL), heparin sulfate (29 μg/mL), human serum albumin (30 mg/mL), trimethoprim (16 μg/mL), sulfamethoxazole (80 μg/mL) and dextran (12 mg/mL for fetal reservoir and 3 mg/mL for maternal reservoir) in deionized water. Sodium bicarbonate was used to adjust the pH to 7.4. Paclitaxel formulations, when added to the maternal perfusion medium, were prepared according to package instructions.

Human placentas were obtained immediately after delivery (Labor and Delivery, John Sealy Hospital) from uncomplicated pregnancies carried to term with no group B

streptococcus, HIV, or other infection. Lobules suitable for perfusion were chosen based on their ease of isolation and the lack of tissue perforation on either the fetal or maternal side. The fetal artery and fetal vein were catheterized, and flow of perfusion medium was established at 3 mL/min (fetal reservoir volume was 150 mL). The lobule was placed on the saline bath apparatus to maintain the placental tissue at 37°C. The maternal side was then catheterized by puncturing the maternal side of the placenta with a catheter. The maternal vein was placed in the chamber to take up maternal medium that had left the placental tissue. The maternal perfusion rate was kept at 12 mL/min (maternal reservoir volume was 250 mL). Paclitaxel formulations (20 μg/mL paclitaxel), as well as antipyrine (20 μg/mL), were dissolved in maternal perfusion medium and perfused through the placenta. Maternal artery, fetal vein, maternal reservoir and fetal reservoir samples were taken at pre-determined time points for the analysis of paclitaxel and antipyrine concentrations. After the completion of a perfusion experiment, perfused lobules were dissected out from the placenta and stored at -80°C for further analysis of accumulated paclitaxel concentrations.

Paclitaxel and antipyrine concentration determination

Concentrations of antipyrine and paclitaxel in placental perfusion medium were determined by reversed-phase high performance liquid chromatography (HPLC). Paclitaxel samples were prepared by liquid-liquid extraction (64,65). Briefly, 250 μL of perfusion medium was placed in a glass tube, and 25 μL of internal standard solution (55 μg/mL celecoxib in acetonitrile) was added. To the test tube, 3 mL of chloroform were added. The contents of the tube were shaken vigorously, and then the aqueous and organic layers were allowed to separate. Of the organic layer, 2 mL were removed and dried at room temperature under a stream of nitrogen. The residue was reconstituted in 100 μL of the initial mobile phase, which was 60% acetonitrile and 40% aqueous formic acid (0.01%

v/v formic acid in water). 50 µL of the reconstituted sample were injected in the HPLC system.

Samples for antipyrine analysis were prepared by protein precipitation. 250 µL of medium containing antipyrine were precipitated in 1 mL of acetonitrile. The mixture was then centrifuged at 20,000 × *g* to pellet the proteins. 100 µL of the supernatant was removed and placed in HPLC vials, and 10 µL of this solution were injected in the HPLC system.

Concentrations of paclitaxel accumulated in placental lobules were also determined by HPLC. Placental tissue (1 g) from each lobule was homogenized in phosphate buffered saline (pH 7.4) at a concentration of 25% w/v. After the tissue was homogenized, 250 µL of the homogenate was placed in a glass test tube. The homogenate was spiked with celecoxib (50 µL of 55 µg/mL in acetonitrile), and then 3 mL of chloroform were added to the test tube. The contents of the tube were shaken vigorously, and the organic layer was allowed to separate from the aqueous layer. Then, 2 mL of the organic layer were placed in a glass vial and then dried under nitrogen. The residue was reconstituted in 100 µL of the initial mobile phase and injected in the HPLC system (50 µL injection volume).

The HPLC system used consisted of a Waters 1525 Binary Pump, 2707 Autosampler, and a 2998 Photodiode array detector (Waters, Milford, MA). The column used was a Kromasil C-18 column (150 x 4.6 mm, 5 µm particle size, 100 Å pore size, Akzo Nobel, Bohus, Sweden). For the detection of paclitaxel, the initial mobile phase was 60% acetonitrile and 40% aqueous formic acid (0.01% v/v formic acid in water). After 7 minutes, the flow changed to 95% acetonitrile over 3 minutes, and remained at 95% acetonitrile for 3 minutes. The flow then reverted to 60% acetonitrile and was allowed to equilibrate for the next sample. Detection of paclitaxel (4.5 minutes) and celecoxib (7.2 minutes) was done at 230 nm. Antipyrine samples were run using an isocratic method consisting of 35% acetonitrile and 65% aqueous formic acid (0.01% v/v formic acid in water). Detection of antipyrine (2.5 minutes run time) was at 243 nm.

Protein concentration of the homogenate was determined by bicinchoninic acid assay (Pierce BCA protein assay kit, Thermo Fisher Scientific, Waltham, Massachusetts). Placental lobule homogenates were diluted into 2% Triton X-100 in water (1:10 dilution). Samples were then incubated at 37°C for 24 hours, and then centrifuged for 5 minutes at 1000 × *g*. The supernatant was taken for protein concentration quantification.

Calculations and statistics

The HPLC methods used for the analysis of placental perfusions was validated for both paclitaxel and antipyrine. Intra-day precision was calculated as the relative standard deviation of six independently processed samples prepared on a single day for three days. Inter-day precision was calculated as the relative standard deviation of the averages of the samples processed on three days. Linear regressions were calculated for standards of both antipyrine and paclitaxel across the necessary concentration range, and were 1/X weighted. From linear regressions, accuracy and linearity (R^2) were determined. Accuracy was calculated as the average of six samples at three concentrations as a percent of the value found from the linear regression. Recovery of paclitaxel at three concentrations was determined to be the peak area of each processed sample as a percent of the peak area of a standard of the compound assuming complete partition into the organic phase during liquid-liquid extraction. Recovery of antipyrine was similarly calculated at three concentrations, but was given as the peak area of a processed sample as a percent of the peak area of a standard assuming complete dissolution of antipyrine into supernatant after protein precipitation. Recovery and intra-day precision were calculated again for media that had been perfused for 30 minutes and 120 minutes to ensure that no substantial differences would be seen in the processing of the samples for the duration of the perfusion.

Fetal transfer rates, reservoir concentrations, and maternal artery concentrations were all calculated as a percent of the initial maternal concentration. Clearance index was

calculated as the fetal transfer rate of paclitaxel divided by the fetal transfer rate of antipyrine at a given time point. All concentrations and clearance indices are given as averages for four perfusions with error bars representing standard deviation. Placental lobule accumulation of paclitaxel was determined as the ratio of the concentration of paclitaxel to the concentration of protein in a particular lobule homogenate sample.

Analysis of variance and Tukey's Post Hoc analysis were used to examine differences between the three treatment groups in fetal reservoir, maternal reservoir, fetal artery, maternal artery, and placental lobule concentrations at 4 hours.

RESULTS AND DISCUSSION

High performance liquid chromatography

The HPLC methods developed for quantification of both paclitaxel and antipyrine concentrations were within the desired limits of accuracy and precision. Linear calibration curves were generated within the necessary range of concentrations (20000 ng/mL for both antipyrine and paclitaxel). The higher concentration in the range, which is the initial concentration used in placental perfusion experiments, was based on the C_{max} of paclitaxel in both Abraxane and Genexol-PM (Taxol was dosed equivalently to avoid concentration dependent differences in results). Paclitaxel was quantifiable down to a concentration of 200 ng/mL (Appendix A.1-A.3), and accuracy at 200, 10000, and 20000 ng/mL were all very close to 100% (Appendix A.4). Based on the peak areas, the lower limit of detection of paclitaxel was 100 ng/mL. This detection limit allowed for an observation of any fetal transfer rate above 0.5%. Intra-day precision values for paclitaxel quantification were all less than 10%. Inter-day precision values were somewhat higher than 10% at the lowest and highest concentrations, but were otherwise considered acceptable. Importantly, recovery of paclitaxel in media that had already been perfused (30 minutes and 120

minutes) varied slightly more at the concentration of 200 ng/mL. This was expected, because in effect the noise would be higher when peak areas are lower (Appendix A.5), due to a change in the matrix (e.g. accumulation of blood).

Antipyrine was detectable at a concentration of 200 ng/mL and quantifiable at a concentration of 500 ng/mL. Assuming adequate overlap between maternal and fetal circulations, antipyrine concentrations should quickly equilibrate to about 50% of the initial maternal concentration. The lower limits of detection and quantification achieved were therefore suitable for the purposes of perfusion experiments (Appendix A.1-A.3). Accuracy of the antipyrine method was very close to 100% at all three concentrations (Appendix A.4). Recovery was very similar across all concentration ranges, and precision values were all below 10%. When tested in the media perfused for 30 minutes and 120 minutes, it appeared that the injections exhibited reduced precision at 500 ng/mL. However, recovery was almost identical to that of pure perfusion medium (Appendix A.5).

Sample stability at 4°C for one week was also tested because all perfusion samples were stored under these conditions for a maximum of one week before analysis. Samples of both paclitaxel and antipyrine stored at 4°C showed almost no differences between days 1 and 8, indicating that both compounds could be stored under these conditions for up to a week or until the samples were ready to be analyzed (Appendix A.6).

The method for determination of placental lobule concentrations of paclitaxel by HPLC also employed celecoxib as an internal standard. This method was linear; however, accuracy and precision of the method was less than the method of extraction from perfusion medium, and baseline noise was higher. This might be due to the higher concentration of different types of proteins and cell membrane components that may not be present in perfusion medium (Appendix A.7).

Fetal transfer rates, clearance indices, and fetal reservoir accumulation

The *ex vivo* dually perfused human placental cotyledon model relies on the use of placentas delivered at term. Inherently, physiology of the placenta changes throughout gestation, including trophoblast cell phenotypes such as syncytialization and receptor expression (66). Inferences can be made from this data in combination with what is known about placental transporter expression. In particular, P-glycoprotein expression has been shown in multiple studies to decrease with gestational age, meaning that the impact of P-glycoprotein on the efflux of paclitaxel may be more pronounced earlier in gestation than may be inferred from term placental studies (14,67).

Transfer of paclitaxel or antipyrine across the placenta from the maternal to the fetal compartment was measured as the fetal transfer rate, which is calculated as the ratio of the concentration at a particular time in the fetal vein to the initial maternal concentration. For perfusions to be considered acceptable, the fetal vein concentration of antipyrine at 120 minutes must be at least 75% of the antipyrine concentration at 120 minutes in the maternal artery, which was an indication of adequate overlap between maternal and fetal circulations. Antipyrine concentrations equilibrated between the maternal and fetal compartments to approximately 50% of the initial maternal concentration in all perfusions (Appendix C). The fetal transfer rate at four hours of paclitaxel in Genexol-PM (17.3%) and Abraxane (15.9%) were on average higher than that of Taxol (13.3%), though variability between perfusions makes it unclear if there were true differences between these groups. This trend was exhibited for the entire four hours of perfusion (Figure 2.4).

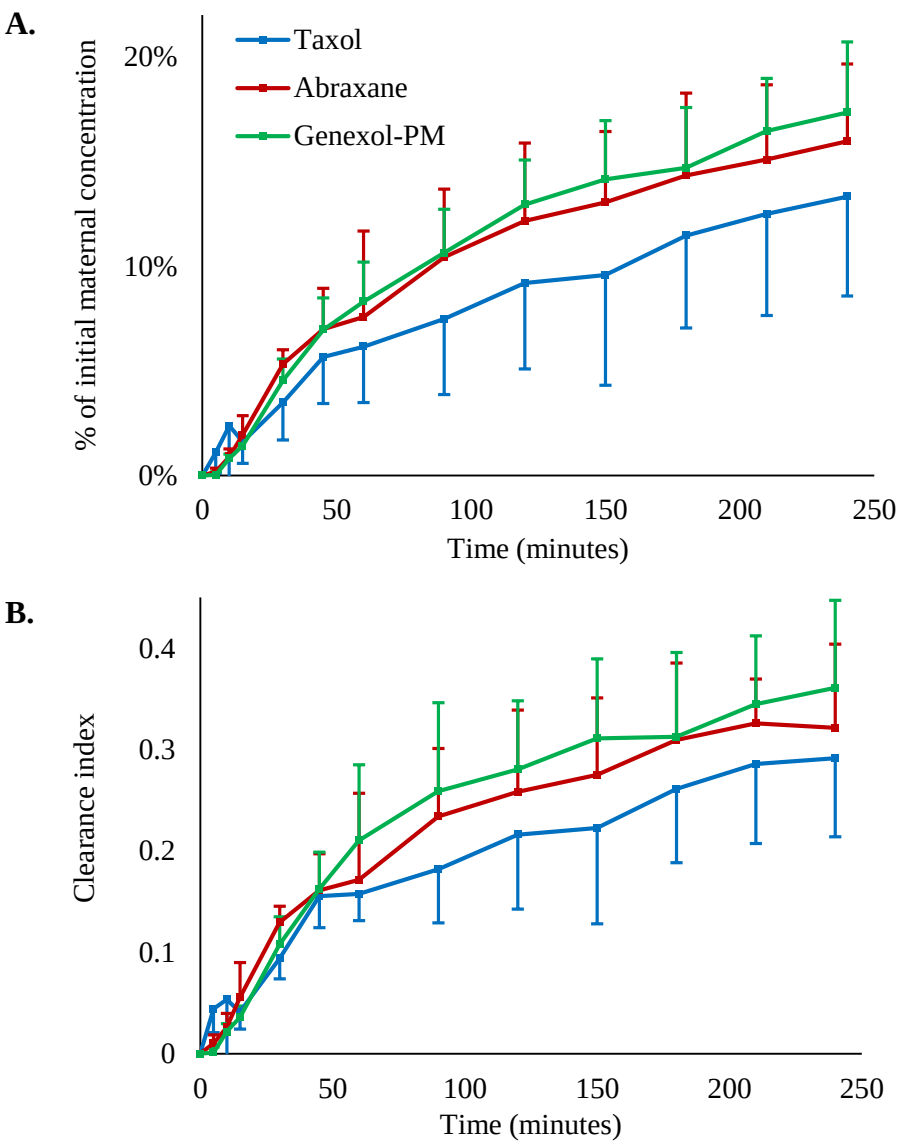

Figure 2.4 Fetal transfer rate and clearance index of paclitaxel formulations

(A) Fetal transfer rates of three formulations of paclitaxel tested. (B) Clearance index of paclitaxel, which is the ratio of fetal transfer rate of paclitaxel to that of antipyrine. Error bars indicate standard deviation (n=4 per group).

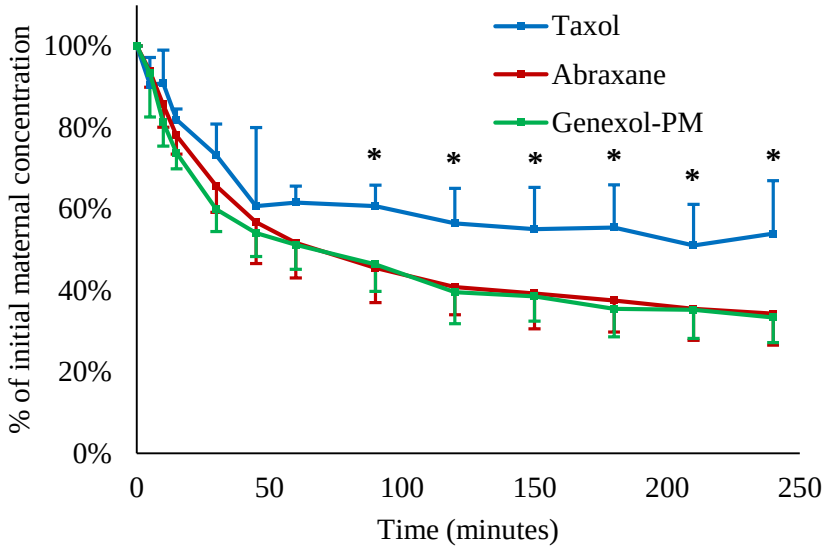

Figure 2.5 Maternal artery concentrations of paclitaxel formulations

Concentration of paclitaxel in maternal artery, sampled over the course of the perfusion experiments. Error bars indicate standard deviation (n=4 per group). Results were analyzed by ANOVA, followed by Tukey's HSD (*, $P < 0.05$).

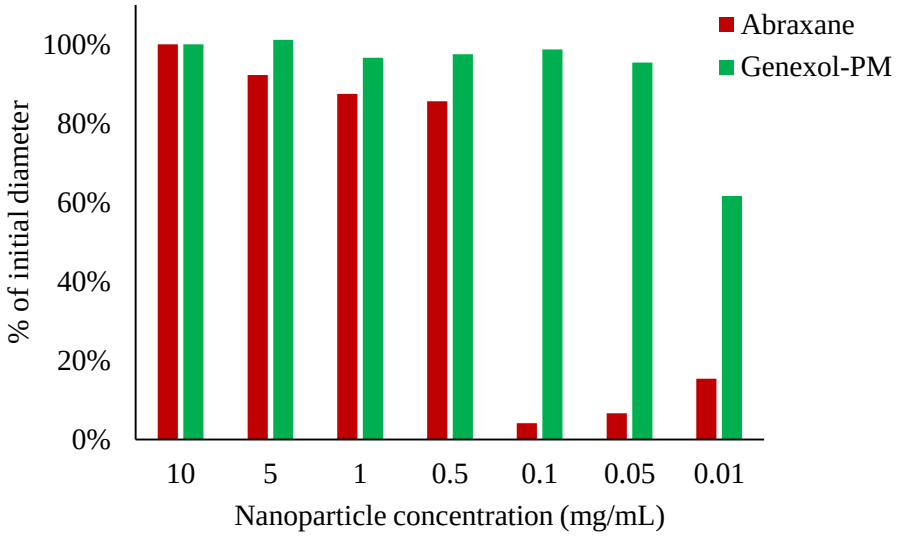

Figure 2.6 Effect of dilution on particle size of nanoformulations

Particle size of both Abraxane and Genexol-PM dissolved in water at various concentrations, measured by dynamic light scattering (based on volume distribution).

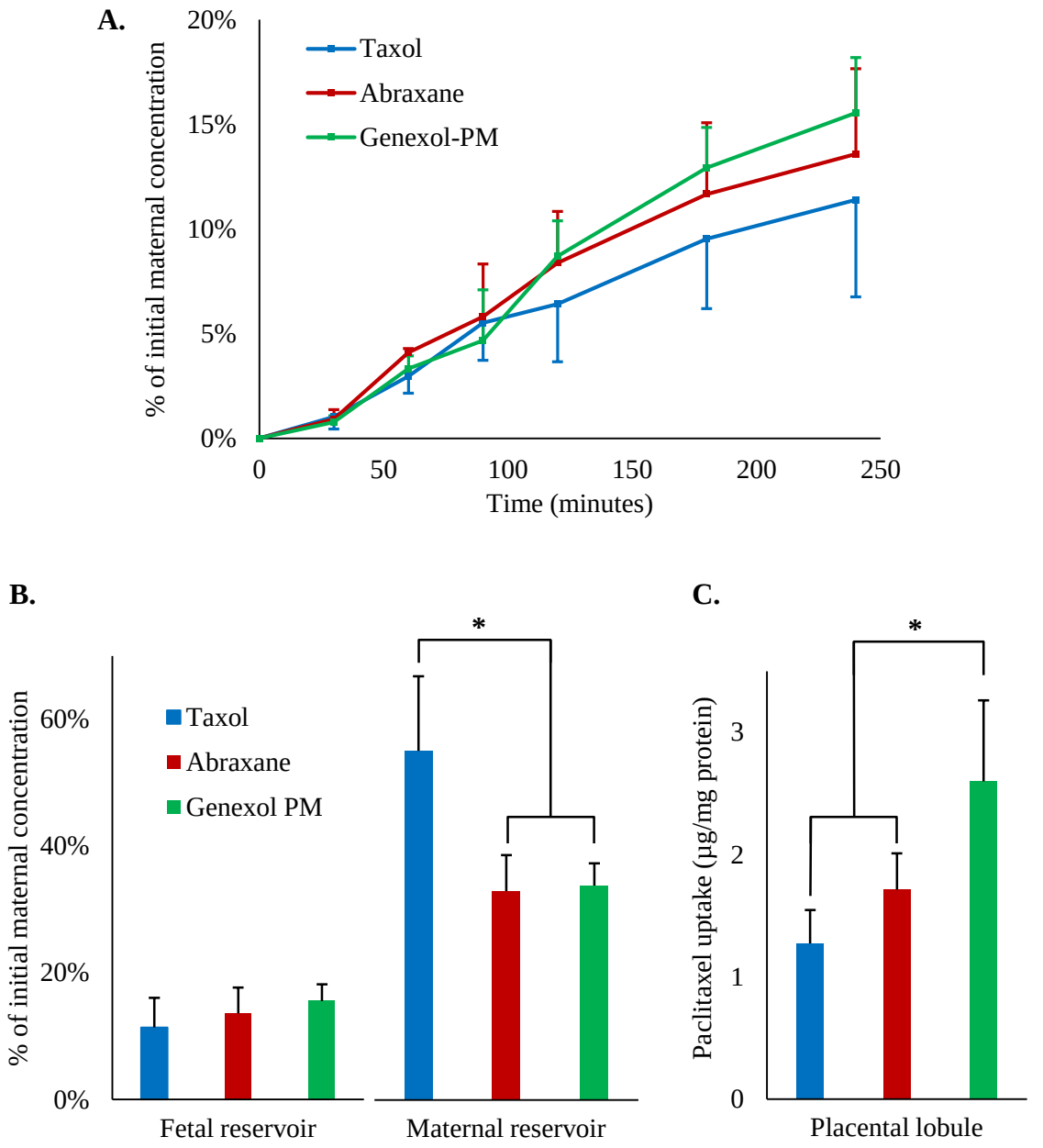

Figure 2.7 Reservoir and lobule concentrations of paclitaxel

(A) Fetal reservoir concentrations of paclitaxel over the course of the perfusion. (B) Fetal and maternal reservoir concentrations at 4 hours of perfusion. (C) Placental lobule concentrations of paclitaxel after 4 hours of perfusion. Error bars indicate standard deviation (n=4 per group). Results were analyzed by ANOVA, followed by Tukey's HSD (*, $P < 0.05$).

Clearance index of paclitaxel, calculated as the ratio of the fetal transfer rate of paclitaxel to that of antipyrine, is used to normalize placentas based on their antipyrine transfer. Antipyrine is a compound that freely diffuses across the placenta and exhibits very little accumulation in the placental tissue. Therefore, differences in fetal transfer rates between placental perfusion experiments that result from differences in the overlap between maternal and fetal circulations can be seen in antipyrine transfer. These differences in fetal transfer rates of a particular compound between placentas can be normalized to antipyrine by dividing the fetal transfer rate of the compound in question to that of antipyrine. Clearance indices between the three formulations exhibited similar trends to the fetal transfer rate. The clearance indices of Genexol-PM (0.36 ± 0.09) and Abraxane (0.32 ± 0.08) were somewhat higher than that of Taxol (0.29 ± 0.08) at four hours, but similar to the fetal transfer rates, the variability between perfusions makes drawing a firm conclusion regarding differences in fetal transfer rates difficult (Figure 2.4). It is likely that both the fetal transfer rate and clearance index of paclitaxel varies little between the three formulations.

Fetal reservoirs in all perfusions were sampled for the duration of the perfusion experiments. Unlike fetal transfer rate, these samples are taken directly from the reservoir and not the fetal vein. Paclitaxel accumulation in the fetal reservoir was higher on average in the perfusions of Genexol-PM and Abraxane (Figure 2.7), but did not appear substantially different, following a similar trend to both clearance index and fetal transfer rate.

Maternal artery concentration and accumulation in maternal reservoir and placental lobule

An important consideration in the transplacental transfer of any xenobiotic or nanomaterial is that the material in question must traverse both the placental trophoblast,

basal membrane, and the fetal capillary endothelium before entering the fetal circulation. Both the placental trophoblast and fetal capillary endothelium have different transporters for efflux and facilitated diffusion (66). In addition to this, substances that cannot diffuse across membranes must undergo endocytosis by the trophoblast before they can enter the tissue or cross to the fetal compartment. As such, knowing the maternal artery and reservoir concentrations of the material is critical in understanding the processes by which drugs or nanomaterials interact with the placenta and the effects they might have. Maternal artery concentrations of both antipyrine and paclitaxel were monitored for the duration of the experiments. Antipyrine concentrations typically quickly equilibrated between maternal artery and fetal vein (Appendix C). Paclitaxel concentrations in the maternal artery varied significantly between the three formulations. As seen in Figure 2.5, Taxol had on average a higher maternal artery concentration after 4 hours of perfusion (53.9% ± 12.9% of initial maternal concentration) compared to Abraxane and Genexol-PM, which performed almost identically for the duration of the experiments (34.3% ± 7.7% and 33.3% ± 6.1% of initial maternal concentration at 4 hours, respectively). In addition, for the majority of the perfusions, it appeared that maternal artery concentration of paclitaxel changed very little (60.7% ± 19.2% at 45 minutes and 53.9% ± 12.9% at 4 hours). Maternal reservoir concentrations were also determined at the end of the perfusions (Figure 2.7). The concentration of paclitaxel remaining in the maternal reservoir was higher in experiments where placentas were perfused with Taxol compared to Abraxane and Genexol-PM, which corresponds to the maternal artery concentrations.

The trends exhibited in the maternal artery and reservoir concentrations of paclitaxel, taken together with the fetal transfer rates of these compounds, suggest that nanoparticle formulations Abraxane and Genexol-PM may have a higher tissue accumulation compared to Taxol. In order to assess the extent of accumulation of paclitaxel from the three formulations in the lobules, tissue concentrations were analyzed by HPLC. An important limitation of the determination of lobule concentrations is that

there is a degree of variability due to some differences between lobules in size and overlapping circulation with other lobules. Therefore, achieving a 100% mass balance can be difficult when a significant portion of the drug accumulates in the tissue. Nonetheless, large differences in lobule concentration can indicate substantial differences between formulations in their behavior. The concentrations of paclitaxel were normalized to protein concentration of tissue (Figure 2.7). Paclitaxel concentrations were significantly higher in placentas perfused with Genexol-PM (2.6 ± 0.7 μg paclitaxel/mg protein) compared to Abraxane (1.7 ± 0.3 μg paclitaxel/mg protein) and Taxol (1.3 ± 0.3 μg paclitaxel/mg protein). These data suggest that encapsulation in Genexol-PM allows paclitaxel to enter the placental tissue more compared to free paclitaxel. Interestingly, Abraxane led to a lower placental tissue accumulation of paclitaxel compared to Genexol-PM. This may be attributed to the release profile of paclitaxel from these nanoformulations. The differences in tissue uptake and maternal concentrations between the three formulations mean that there is a likely a large influence of the composition of the formulation on the interaction of the drug with the placenta.

Abraxane has long been known to be an immediate release formulation. More specifically, it has been shown to that Abraxane breaks down upon dilution to the C_{max} concentration in plasma that is achieved upon administration to patients, which is approximately 20 μg/mL (51). We have also shown by dynamic light scattering the disappearance of the albumin nanoparticles in Abraxane when it is diluted from 0.5 mg/mL to 0.1 mg/mL in water, which corresponds to a dilution of 50 μg/mL to 10 μg/mL of paclitaxel in the formulation (high performance particle sizer, Malvern). Therefore, it is reasonable to conclude that the nanoparticles are no longer intact upon dilution into perfusion medium. Instead, the drug most likely behaves like free paclitaxel bound to albumin. The change in albumin concentration due to Abraxane is minimal, because perfusion medium contains 30 mg/mL albumin and the concentration of Abraxane administered in perfusion experiments is 200 μg/mL. Interestingly, administration of

Taxol in perfusions resulted in much higher maternal concentrations of paclitaxel than perfusions with Abraxane. The tissue accumulation of Abraxane was marginally higher, but considering the variability in the HPLC method and between experiments, it is difficult to say that there was a true difference in the resulting tissue accumulation. Taken together, it is most likely that Cremophor-EL, which is present in the perfusions of Taxol at a concentration of 0.33% v/v), plays a role on the ability of paclitaxel to enter the placental tissue. This is likely due to a shift in the partition coefficient of paclitaxel between the cell membrane and the perfusion medium towards the medium due to its lipophilic nature.

The differences in maternal artery and maternal reservoir between Taxol and Genexol-PM were also quite substantial, and taken with lobule concentrations indicates that Genexol-PM indeed causes a robust increase in the placental uptake of paclitaxel. Genexol-PM is undergoing investigation for bioequivalence to Abraxane. The property of Genexol-PM to disintegrate in plasma in a similar manner to Abraxane is part of the basis of this study (55). However, it has been shown that Genexol-PM may exhibit sustained release in phosphate buffered saline (33). We have also shown that upon dilution in water, the micelles are intact at 50 μg/mL (corresponding to approximately one quarter of the C_{max} paclitaxel). Due to the limitations of dynamic light scattering, it is difficult to say if this phenomenon occurs in placental perfusion medium as well. However, in conjunction with the approximately two-fold higher paclitaxel concentration in the tissue treated with Genexol-PM, it is likely that micelles are indeed intact and can accumulate in the placental tissue, causing an increase in the accumulation of paclitaxel. The phenomenon of overcoming placental efflux by nanoencapsulation of drugs has been shown in BeWo cells previously (48).

CONCLUSION

The placental perfusion experiments shown here make a case for differences between formulations in terms of their placental accumulation and their transplacental permeability. There is a degree of variability between placentas in terms of size and, potentially, transporter expression. These differences may have masked differences in the fetal transfer rates between the three perfusions, but it is nonetheless likely that efflux capabilities of the placenta play a role in the passage of paclitaxel to the fetal circulation. In addition, it is evident by both placental lobule concentrations and end perfusion maternal artery and reservoir concentrations that placental accumulation of paclitaxel from nanoparticles is likely higher than that of Taxol. In particular, Genexol-PM appears to cause quite a substantial increase in lobule concentration of paclitaxel, while Cremophor-EL may reduce this effect. This is in agreement with previous studies that have shown that nanoencapsulation of P-gp substrates may shield them from efflux (48). Genexol-PM appears to cause a significant amount of accumulation of paclitaxel in the placenta, though this may not necessarily translate to higher transfer to the fetal circulation. Contrary to our initial hypothesis, Abraxane did not appear to reduce the fetal transfer rate of paclitaxel. Abraxane behaved very similarly to Genexol-PM in maternal circulation, with a substantial reduction in concentration compared to Taxol. This difference, too, is most likely due to alterations in paclitaxel partitioning into the cell membranes as a result of Cremophor-EL. Overall, it appears that type of nanoformulation may influence the total fetal exposure to paclitaxel and, perhaps more significantly, placental accumulation. These may play therefore play a role in fetal and placental health. Further studies will include an investigation of the propensity of the different types of nanoparticles to accumulate in the placenta, the ability of P-gp to efflux paclitaxel when formulated as Abraxane and Genexol-PM, as well as the mechanisms of endocytosis employed for entry into the trophoblast.

Chapter 3. Uptake and efflux mechanisms of paclitaxel formulations

INTRODUCTION

As mentioned in Chapters 1 and 2, encapsulation in nanoparticles can potentially have a large effect on the way that a particular drug interacts with biological barriers. Free drugs may undergo many different cellular mechanisms of uptake, whether by endocytosis or relying on transporter proteins. If the drug is unable to interact with these cellular mechanisms, or if the material that makes up the nanoparticle interacts with a cell in a way that the drug does not, then the measureable parameters such as permeability or cellular uptake may be altered (40,41). As an example, if a drug is subject to efflux by a placental efflux transporter, but is encapsulated in a nanoparticle, the drug is effectively shielded from efflux (48). Also, if the nanoparticle undergoes cellular uptake by recruiting mechanisms of clathrin- or caveolae-mediated endocytosis, or other form of endocytosis, then they may effectively carry the drug encapsulated within them across the cellular membrane. Different examples of these phenomena occurring have been reported in different types of epithelial cells that comprise biological barriers, including placental trophoblast (41,52,68).

The placenta serves as a barrier to potentially harmful xenobiotics, and as such possesses a host of efflux transporters that effectively prevent the transfer of those compounds to the fetus. The placental trophoblast, which was alluded to in Chapter 2, an epithelial layer on the placenta that is the first cellular barrier for compounds and nanoparticles going from the maternal circulation to fetal circulation, is responsible for most of the protective efflux mechanisms (27,69,70). It has been shown on many occasions that paclitaxel can undergo efflux from the placental trophoblast by P-glycoprotein, and that this process can be inhibited by other substrates of P-glycoprotein, such as the compounds verapamil or GF120918 (60).

It has been known for some time that some nanoparticles can cross the placenta in multiple models. Due to the relatively large size of nanoparticles compared to small molecules, it is reasonable to attribute their transplacental passage largely to endocytosis. Placental uptake and transport of nanoparticles are governed by size and material. For example, though polymeric nanoparticles are able to transport across the placenta and may improve the permeability of some drugs across the trophoblast, liposomal formulations may have an opposite effect on transplacental transport (46,47,71).

Endocytosis mechanisms in the placental trophoblast have also been studied, albeit not extensively in the context of nanoparticles. These mechanisms have been shown to be recruited in the case of some small molecules and proteins (52,68). Clathrin heavy and light chains, which are the constituents of clathrin-coated pits; Megalin, a cell surface marker involved in some mechanisms of endocytosis; and caveolin-1 and caveolin-2, protein constituents of caveolae; have all been shown to be expressed in the placental trophoblast (52,72–74). Other mechanisms of endocytosis, such as phagocytosis, may also be employed in nanoparticle uptake as well, but their role in nanoparticle uptake has not been elucidated. It is important to realize that the proteins involved in these uptake mechanisms are also very likely involved in other functions. For example, clathrin may play a role in cell migration, and similarly, microtubules (which are involved in phagocytosis) are involved in cell division (72). Caveolin proteins are likely involved in placental trophoblast syncytialization (75).

One of the studied properties of Abraxane and its interaction with endothelial cells is that, upon degradation, albumin-bound paclitaxel can bind to Albondin (gp60), which is a 60 kDa glycoprotein. Gp60 can bind caveolin within the cell, causing membrane invagination and ultimately leading to transcytosis of the albumin-bound drug (32). An additional mechanism that may lead to increased accumulation in some tumors is the binding of albumin to osteonectin (SPARC), which is overexpressed and secreted by some tumor types. It is proposed that upon caveolae-mediated transcytosis of albumin across the

endothelium, it can bind SPARC and be retained within the tumor tissue (76). The placental trophoblast is, however, a unique epithelial cell layer that differs substantially from endothelial cells. It is not known if transcytosis of albumin-bound drugs can occur in placental trophoblast, but it has been shown that the transfer of paclitaxel in placental perfusions in the presence of physiological concentrations of albumin (30 mg/mL) is less than when compared to perfusions with reduced concentrations (2 mg/mL) (15). Also, as mentioned previously, proteins that appear to be involved in the uptake of albumin into trophoblast cells include clathrin and megalin. Also, trophoblast uptake of albumin does not necessarily result in transcytosis (52,74).

The efflux transporters present on the placental trophoblast, as well as the endocytosis mechanisms that these cells can use, will largely govern the transfer of the nanoformulations of paclitaxel we have examined in this project. It is critical to begin to understand these mechanisms and how they are involved in nanoparticle transport in the placenta, especially in the context of new nanoparticle drug formulations entering the market. The model chosen for the studies shown here is the BeWo cell line, a choriocarcinoma cell line that has been used extensively as a model of the placental trophoblast. These cells can be grown on collagen-coated semi-permeable membranes, where they can form tight junctions. They can then be used for drug and nanoparticle transport and uptake studies (47,77). P-glycoprotein, clathrin, megalin, and caveolin are known to be present and functional in BeWo cells. We designed these experiments to probe the mechanisms that we were interested in using pharmacological inhibitors of P-glycoprotein efflux and various mechanisms of endocytosis.

MATERIALS AND METHODS

Materials

N,N-Dimethylformamide (DMF), dimethyl sulfoxide (DMSO), dichloromethane, tetrahydrofuran (THF), NHS-fluorescein, dibasic sodium phosphate, and ethylene diamine tetraacetic acid disodium salt (EDTA) were purchased from Fisher Scientific. DMEM/F-12 and HBSS were purchased from Corning (Corning, NY). Fetal Bovine Serum was purchased from Hyclone (Little Chalfont, UK). Non-essential amino acids, L-glutamine, antibiotic/antimycotic, and trypsin/EDTA solutions were purchased from Gibco (Waltham, MA). Verapamil hydrochloride and filipin complex were purchased from Sigma Aldrich. 7-Methoxycomarin-3-carbonyl azide was purchased from Chemodex (St. Gallen, Switzerland). Chlorpromazine hydrochloride was purchased from Chem-Impex International, Inc. (Wood Dale, IL). Methoxypolyethylene glycol-*b*-poly(D,L)lactic acid (mPEG-PDLLA, MW: 2247/1575 by NMR) was purchased from PolySciTech (West Lafayette, IN).

Synthesis of fluorescent polymeric micelles

Conjugation of 7-methoxycoumarin-3-carbonyl azide (7-MC) to mPEG-PDLLA was conducted under inert conditions, as described previously (78). Briefly, a flame-dried Schlenk flask was purged with nitrogen, after which the dry mPEG-PDLLA (104 mg, 0.027 mmol) and 7-MC (36 mg, 0.163 mmol) were added to the flask against a nitrogen counterflow. The flask was purged with nitrogen again, and 10 mL of anhydrous dimethylformamide (DMF) were added to the flask through a rubber septum. The reaction was allowed to take place at 80°C for 5 hours under positive pressure of nitrogen. The reaction solution was then allowed to cool to room temperature, and then the product was precipitated in ice-cold diethyl ether and then vacuum filtered (0.22 μm), dried, and

weighed. Size exclusion chromatography (Appendix D.2) was performed using an SB-804HQ column (Shodex) on the HPLC system described in Chapter 1, with a mobile phase flow rate of 0.7 mL/min (50:50 ACN:water) and fluorescence detection (ex: 330 nm, em: 402 nm) using a 2475 Multiwave Fluorescence Detector (Waters).

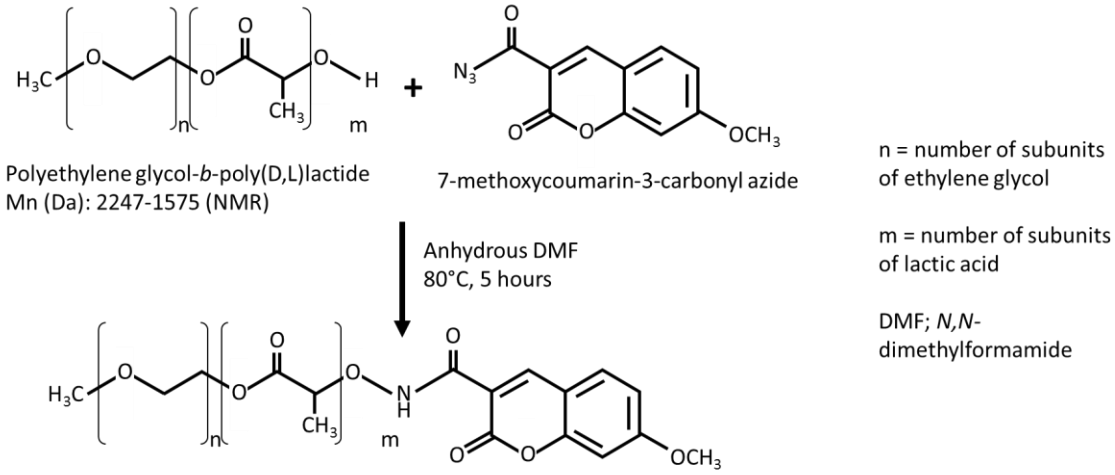

Figure 3.1 Reaction of PEG-PDLLA with 7-methoxycoumarin-3-carbonyl azide

To prepare micelles, the dried product was dissolved in tetrahydrofuran (THF), along with unconjugated mPEG-PDLLA, to give a final dye concentration of 3% w/w, at a final concentration of 20 mg/mL in THF, yielding a turbid solution. This solution was then added dropwise to deionized water (10:1 water:THF). The resulting clear solution was placed on a rotary evaporator at 70°C under vacuum to remove THF. The solution was passed through a 0.22 μm filter, lyophilized, and stored at -20°C, desiccated. Particle sizes of the micelles before and after lyophilization, as well as unconjugated polymeric micelles, were measured by dynamic light scattering using a high performance particle sizer (HPPS, Malvern), shown in Appendix D.3.

Synthesis of fluorescent albumin nanoparticles

Human serum albumin (HSA) was first conjugated to NHS-fluorescein, to prepare fluorescent HSA (fHSA). HSA (61 mg, 9.2E-4 mmol) was dissolved at 6.1 mg/mL in 150 mM sodium chloride in deionized water, buffered with dibasic sodium phosphate (20 mM) at a pH of 8.5. NHS-fluorescein (6.7 mg, 0.014 mmol), dissolved in dimethylsulfoxide (DMSO) at 10 mg/mL was then added to the solution of HSA. The reaction solution was allowed to shake at 0°C for 2 hours. After 2 hours, the solution was dialyzed against deionized water for 6 days at 4°C (changing water every hour for the first four hours, then once per day) to remove the majority of the excess dye. This product was further purified by size exclusion chromatography using PD-10 columns, which are loaded with Sephadex™ G-25 medium (GE Healthcare). The resulting solution was lyophilized and stored at -20°C, desiccated. Absence of free dye in the product was determined by polyacrylamide gel electrophoresis (SDS-PAGE) and densitometry using an AlphaImager 2200 (Alpha Innotech) using a UV lamp (365 nm) for excitation and a 537 nm filter for emission (Appendix D.1).

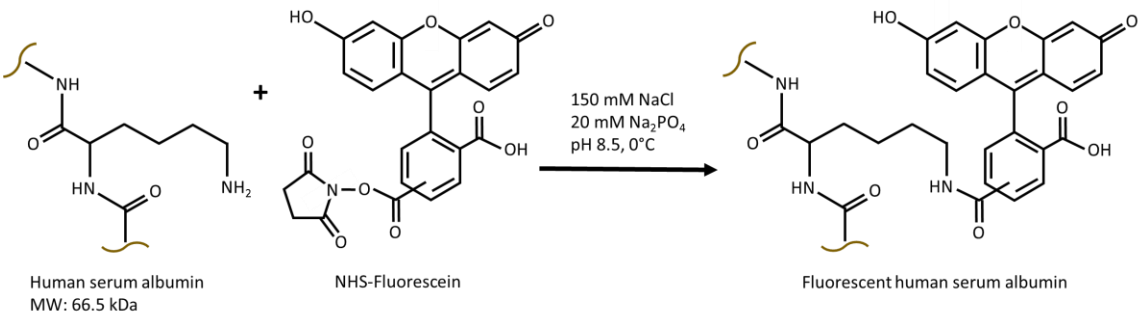

Figure 3.2 Reaction of human serum albumin with NHS-fluorescein

Nanoparticles were prepared from fHSA by mixing fHSA (1% w/w) with unconjugated HSA, and dissolving in deionized water (2.5% w/v, 8 mL). To this solution, 2 mL of dichloromethane was added. The suspension was then sonicated (XL-2000 ultrasonicator with P-1 probe, Misonix, Farmingdale, NY) at 0°C for a total of 8 minutes (30 seconds on, 30 seconds off). After sonication, the dichloromethane was removed from the nanoparticles by rotary evaporation under vacuum for 30 minutes at 35°C. The resulting nanosuspension was passed through a 0.45 μm filter and lyophilized. Particle size of the nanoparticles was measured by dynamic light scattering (Appendix D.3).

Transport studies

BeWo (b30 clone, passage 28-35) cells were grown in 50:50 DMEM:F-12 media (with phenol red) supplemented with 10% fetal bovine serum, L-glutamine, non-essential amino acids, and penicillin/streptomycin, at 37°C (95% humidity, 5% CO_2). At 70-80% confluence, cells were trypsinized and seeded in the apical well of Transwell™ plates (12 wells/plate, polycarbonate membrane, 3 μm pore size, Corning) that were coated with human placental collagen at a concentration of 224,000 cells/mL (0.5 mL in apical chamber, 1.5 mL media in basolateral chamber), and media was changed every two days. Three Transwell inserts were prepared with collagen for each treatment that were not coated with cells, and used to control for permeability differences due to the membrane alone. Transepithelial electrical resistance (TEER) values were measured using an EVOM2 voltohmmeter connected to Endohm-12 electrodes (World Precision Instruments, Sarasota, FL), and cells were used for study when their TEER values were 45-75 $\Omega \cdot cm^2$, which was 7-9 days post-seeding.

Once cells reached the appropriate TEER values, they were used for transport studies. Treatments were prepared in complete media (or HBSS in the case of fluorescent nanoparticle studies) and administered in the apical chamber. Cells treated with fluorescent

particles were gently washed once with HBSS prior to administration of treatments. All paclitaxel formulations were administered at 20 μg/mL. Nanoformulations (Abraxane and Genexol-PM) were prepared in saline according to package instructions. Paclitaxel was dissolved in DMSO prior to administration (final concentration of DMSO 0.1%). Verapamil hydrochloride was dissolved in deionized water and diluted into cell culture medium (100 μM). Fluorescent nanoparticle treatments were prepared at the same concentration as their paclitaxel-loaded counterparts (Abraxane and Genexol-PM). Samples were taken from the basolateral chamber at pre-determined time points and analyzed either by HPLC for paclitaxel concentrations (using the same method described in Chapter 1, adopted for cell culture media) or by fluorescence plate reader (FLx800, BioTek) with filters for 7-MC (λ_{ex}: 340/30 nm, λ_{em}: 400/30 nm) and fluorescein (λ_{ex}: 485/20 nm, λ_{em}: 528/20 nm).

Calculations and statistics

Standard curves were generated for paclitaxel quantification by HPLC based on a 1/X weighted linear regression. Precision was calculated at 3 concentrations as the relative standard deviation of 6 injections. Accuracy was calculated at the same 3 concentrations as the percent difference between the standard curve and the sample (Appendix B.1). Similarly, standard curves were generated for 7-methoxycoumarin-3-carbonyl azide and NHS-fluorescein in both cell culture media and cell lysate (Appendix B.2, B.3). The quality of linear regressions generated for standard curves was determined by their R^2 values.

Permeability across BeWo cells in Transport studies was calculated for paclitaxel and fluorescent nanoparticles by Equation 3.1, where ΔQ is total mass flux of the drug or nanoparticle, Δt is the amount of time that has passed since initiating treatment, C_0 is the

initial concentration of the drug or nanoparticle, and A is the surface area of the Transwell (47).

Equation 3.1

$$P = \frac{\Delta Q / \Delta t}{C_0 \cdot A}$$

Permeability of each formulation was calculated across Transwells containing BeWo cells (P_{cells}), as well as Transwells that were coated with collagen but contained no cells (P_{blank}). From these values, the apparent permeability (P_e) was calculated (equation 3.2).

Equation 3.2

$$\frac{1}{P_e} = \frac{1}{P_{cells}} - \frac{1}{P_{blank}}$$

Apparent permeability across BeWo cells of paclitaxel formulations and fluorescent nanoparticles are given as the averages of the apparent permeability of each well in the study, with error bars representing the standard deviation between each one. The student's t-test was used to examine statistical differences between two groups, whereas analysis of variance, followed by Tukey's Post Hoc test, was used to examine differences between three or more groups.

RESULTS AND DISCUSSION

Effect of P-gp inhibition on paclitaxel formulation permeability

BeWo cells (b30 clone) were used for transport studies. These cells are a choriocarcinoma cell line that is known to express P-gp, which prevents the transplacental transfer of many substrates including paclitaxel. By competitively inhibiting P-gp and

examining the differences in permeability of different formulations, one can ascertain with reasonable confidence the role of P-gp on the efflux of each particular formulation. However, it is critical to understand the limitations of this type of experiment. Inherent limitations of inhibition of mechanisms of efflux (or endocytosis) largely have to do with other cellular functions that may be altered as a result of those pathways being partially or completely blocked. For example, though paclitaxel is known to inhibit microtubule disassembly which may prevent phagocytosis, this action has effects on many other cellular functions including cell division. For this reason, compounds were chosen that demonstrate robust properties of inhibiting specific pathways in multiple cell types, and that yield reproducible results. Also, since paclitaxel is known to be a cytotoxic drug, a lactate dehydrogenase release assay (LDH assay) was performed in BeWo cells to examine the cytotoxicity of paclitaxel and its various formulations at the tested concentrations. No appreciable toxicity was observed in any of the formulations tested, or in DMSO, which was used as a carrier for paclitaxel (Appendix E.1, E.3).

BeWo cells grown on Transwell plates exhibit tight junction formation, which can be measured by TEER values. Transwells were arranged to have similar TEER values between all groups, to ensure that differences between groups are not due to differences in tight junctions. P-gp was inhibited competitively by verapamil, which has been used in previous studies to inhibit P-gp efflux of a number of substrates and in a number of cell lines and models, including BeWo cells and other trophoblast cells (14,48,61,69,79). Indeed, there was a substantial increase in paclitaxel permeability across BeWo cells when treated with 100 μM verapamil (Figure 3.3). Similar studies were conducted with the three formulations of Taxol, Abraxane, and Genexol-PM. In order to ensure that this increase in permeability was not due to cytotoxicity resulting in monolayer gaps, the LDH assay was performed by incubating verapamil for two hours with BeWo cells. No toxicity was observed (Appendix E.2).

Overall, the average permeability across BeWo cells increased when the formulations were co-administered with verapamil, compared to being administered by themselves, but for Taxol and Genexol-PM these differences were modest and not statistically significant. These findings mirror the findings of the perfusion experiments shown in Chapter 2. It is possible that a robust increase in paclitaxel permeability in the Taxol group was not observed due to alteration of paclitaxel to partition into the cell membrane when compared to free paclitaxel. Also, it is possible that the efflux of paclitaxel by P-gp was attenuated in the Genexol-PM group if some of the drug was able to enter the cell while still being encapsulated in micelles. Unlike these formulations, paclitaxel exhibited a two-fold increase in permeability in the presence of verapamil when administered in the formulation Abraxane. This is an indication that this formulation likely behaves most like the free drug paclitaxel, which is consistent with the findings in perfusion studies and reflects the immediate release quality of this nanoformulation.

BeWo cell transport studies have proven in the past to be a very robust and reproducible model for examining transport and efflux mechanisms of placental trophoblast. Importantly, these results do not necessarily represent the entire placental tissue, of which trophoblast cells are only one component. Fetal endothelial capillaries are also known to express certain membrane transporters, but their role in paclitaxel or nanoparticle transport to the fetal circulation are currently unknown (66,80).

Preparation of fluorescent nanoparticles for transport studies

In order to determine the role of nanoparticles in the uptake of paclitaxel into the placental trophoblast, as well as the mechanisms of transport to the fetal compartment, we synthesized fluorescent nanoparticles similar in characteristics to both Abraxane and Genexol-PM. Fluorescent albumin nanoparticles were synthesized from human serum

albumin that was conjugated to NHS-fluorescein. The resulting bond between NHS-fluorescein and lysine present on albumin is an amide. The amount of residual free dye present in the fluorescent albumin was quantified by SDS-PAGE. Free dye migrated slightly faster than bromophenol blue, and was quantified by densitometry. The fluorescent signal attributed to fHSA in the nanoparticle preparation used was 98%, with free dye being less than 2%.

The method of synthesis of Abraxane is not currently public; however, patent information by the makers of Abraxane lists methods of synthesis of albumin nanoparticles which include high pressure homogenization and sonication. Fluorescent albumin nanoparticles were synthesized by sonication in a similar manner to the method described in the patent, with variations made to achieve the desired particle size. An elaboration of fluorescent albumin nanoparticle synthesis can be found in Appendix D.3.

Fluorescent micelles were prepared by labeling mPEG-PDLLA with 7-MC, the result of which is the formation of an amide bond. The polymer used was chosen based upon its similarity to literature values of the molecular weights of the polymer blocks in Genexol-PM. Upon precipitation and filtration, the fluorescent signal attributed to either free dye or low molecular weight dye conjugates was less than 15%, which was appropriate for our studies (Appendix D.2). Additionally, we were able to show that micelle formation occurred for both 7-MC labeled polymer as well as unlabeled polymer, and the particle size remained the same after lyophilization.

Fluorescent nanoparticles were compared to their marketed formulation counterparts in terms of size distribution and degradation characteristics (Figure 3.4). The size distribution of both fluorescent nanoparticles matched very closely with Abraxane and Genexol-PM, and polydispersity indices were within acceptable limits (Table 3.1). Their cytotoxicity was also examined by LDH assay, and no appreciable toxicity was observed (Appendix E.1). We showed in chapter 2 that Abraxane appears to degrade upon dilution to 100 μg/mL, while Genexol-PM remains as micelles down to 50 μg/mL, after which the

particle size appears to decrease. The albumin nanoparticles synthesized did not disintegrate upon dilution like Abraxane. The particles remained intact down to the lowest concentrations tested. This is potentially due to differences in the synthesis method or a change in the characteristics of albumin as a result of the conjugation of fluorescein. These nanoparticles degrade upon incubation at 37°C in HBSS for 20 minutes, however, where 39% of the size distribution by volume was attributed to fragments less than 100 nm in diameter. This is an indication that during the course of the experiment, it is likely that the nanoparticles would degrade in a similar manner to Abraxane. Fluorescent micelles appeared to have a reduction in their diameter at similar concentrations to those observed for Genexol-PM, indicating that dye conjugation likely had little effect on the critical micelle concentration of the polymer (Figure 3.4).

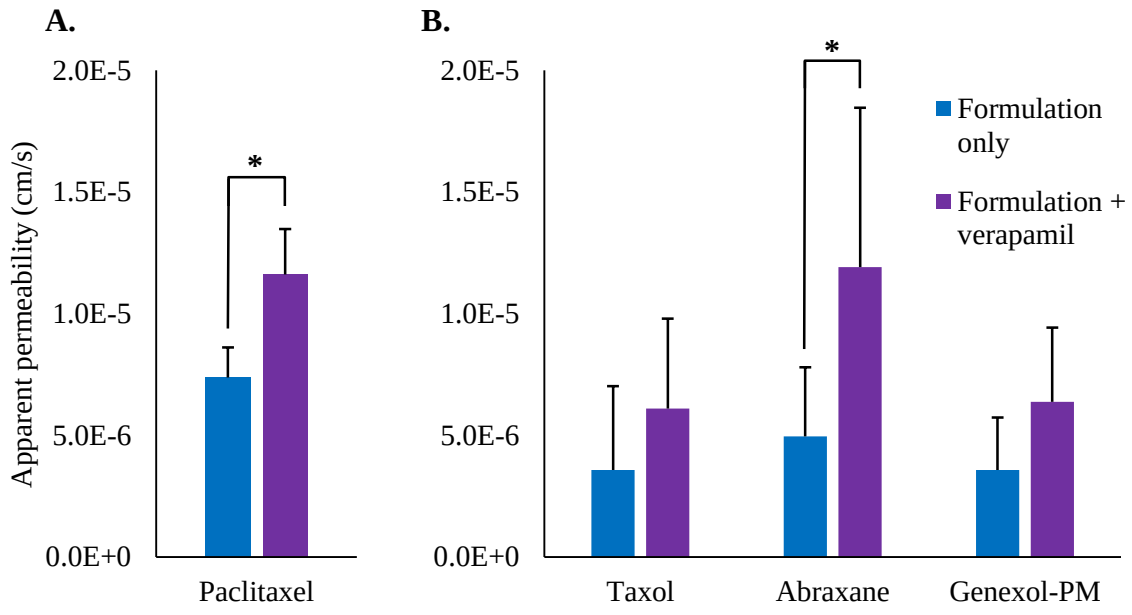

Figure 3.3 Effect of verapamil on paclitaxel permeability across BeWo cells

(A) Permeability of paclitaxel (0.01% DMSO in media) across BeWo cells at 2 hours (n=3). Results analyzed by Student's t-test (*, $P < 0.05$). (B) Permeability of paclitaxel formulations across BeWo cells at 2 hours (n=6 or 7). Results analyzed by ANOVA, followed by Tukey's HSD (*, $P < 0.05$). All error bars indicate standard deviation.

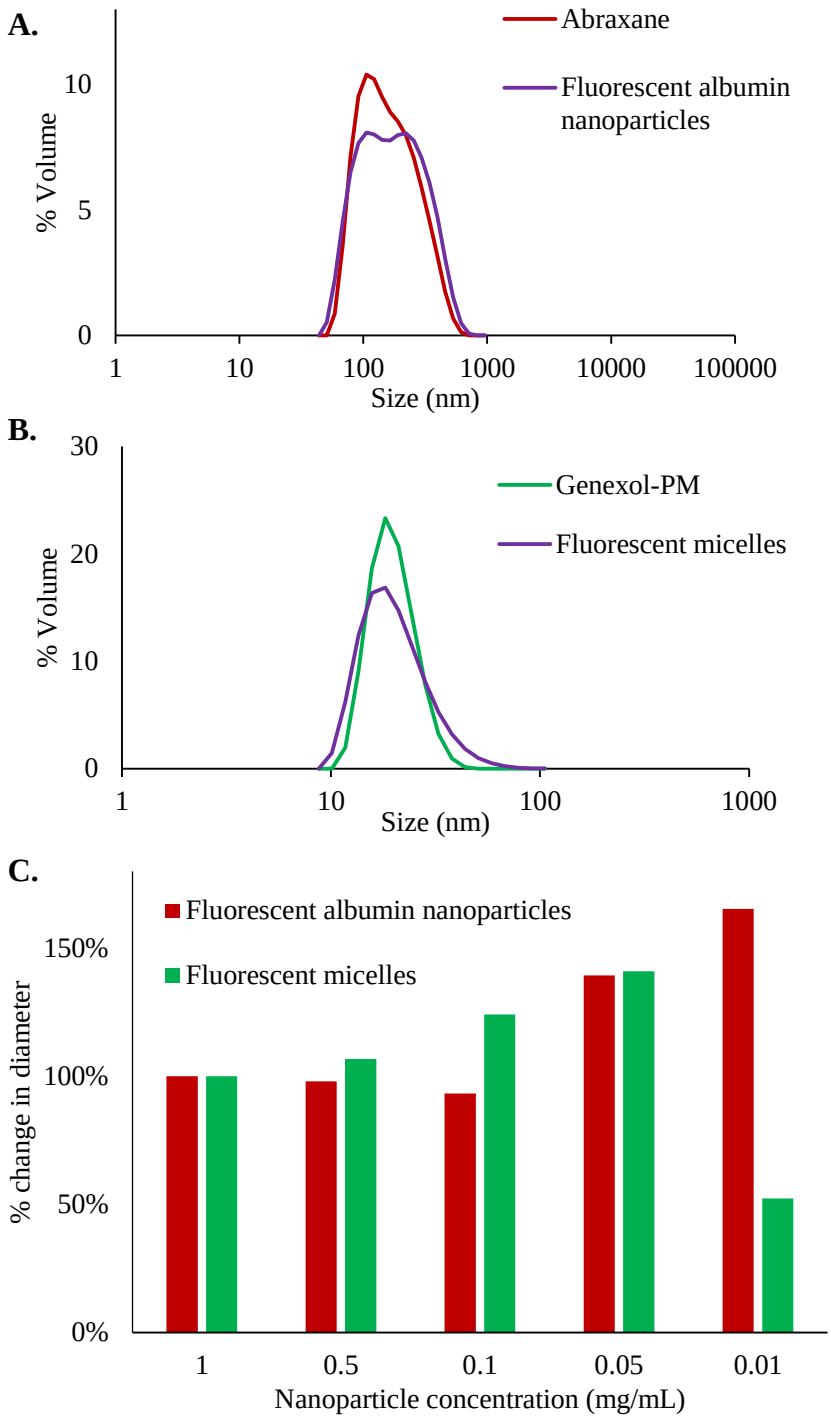

Figure 3.4 Size distribution of Abraxane, Genexol-PM, and fluorescent nanoparticles

(A) Size distribution by volume of fluorescent albumin nanoparticles overlaid on that of Abraxane. (B) Size distribution of fluorescent micelles overlaid on that of Genexol-PM. (C) Effect of dilution on particle size of fluorescent nanoparticles (volume distribution).

Permeability of fluorescent nanoparticles across BeWo cells

Permeability of fluorescent nanoparticles across BeWo cells was examined using HBSS instead of cell culture media due to the background fluorescent properties of complete media (81). Transport studies conducted in BeWo cells demonstrated that, in stark contrast to paclitaxel permeability, different types of nanoparticles have vastly different permeabilities (Table 3.2, Abraxane and Genexol-PM permeability from figure 3.3. added for comparison). The permeability of fluorescent micelles was an order of magnitude higher than that of albumin nanoparticles, indicating that these different materials likely have very different mechanisms of endocytosis and transcytosis.

As a further examination of these differences, these nanoparticles were also co-administered with a number of endocytosis inhibitors, as well as paclitaxel, in order to see where these differences may lie. These compounds were shown not to have appreciable cytotoxicity by LDH assay (Appendix E.3). Permeability of fluorescent albumin nanoparticles was compared to free fHSA that was not made into nanoparticles, and their permeabilities were almost identical at 2 hours. This is expected since the fluorescent nanoparticles degrade within the first 20 minutes of incubation at 37°C in HBSS.

Fluorescent albumin nanoparticles were co-administered with paclitaxel, filipin complex, and chlorpromazine. Paclitaxel (20 μg/mL) is present in the formulation of Abraxane, and since it is able to interfere with microtubule disassembly and is ultimately cytotoxic, it can potentially have an effect on albumin transport across the placenta. Filipin complex (3μg/mL) is a widely-used inhibitor of caveolae-mediated endocytosis. It functions by sequestering membrane cholesterol that is critical for membrane invagination during caveolae-mediated endocytosis. Importantly, this mechanism of action likely has a number of other effects on cellular function, including, potentially, interference with other endocytosis mechanisms (49,82–85). Chlorpromazine (10 μg/mL) is a widely used clathrin-mediated endocytosis inhibitor, which functions by preventing clathrin-coated pit

assembly on the cell membrane. The clathrin-coated pits then become sequestered by intracellular vesicles (52,86,87). None of the inhibitors caused differences in permeability across BeWo cells of fluorescent albumin nanoparticles (Figure 3.5). Uptake into BeWo cells was also similar across all groups. Co-administration of Filipin resulted in the lowest average albumin uptake, but due to variability in the uptake measurements it is unclear if these experimental differences are true (Figure 3.6). Therefore, these studies were unable to elucidate precise mechanisms of uptake and transport of albumin nanoparticles. Other methods of examining these mechanisms, including knockdown of key proteins involved in each pathway, may be an alternative method of examining these mechanisms.

Fluorescent micelle endocytosis and transport mechanisms were also probed using these mechanistic inhibitors. No differences were seen between the groups in either permeability or uptake, indicating that these micelles may not cross the trophoblast by these particular mechanisms.

Fluorescent micelles were also co-administered with EDTA (10 mM). EDTA is known to chelate divalent cations in aqueous solution, but it can also cause increases in paracellular transport by the reduction of tight junction formation. This phenomenon has been widely exploited in epithelial cell culture studies (88). EDTA co-administration led to an increase in the permeability of fluorescent micelles across BeWo cells, indicating that the micelles were likely not passing through the cell layer by a paracellular route.

Table 3.1 Particle sizes and polydispersity indices of nanoparticles

	Z-average particle size (nm)	PDI
Abraxane	156.2	0.13
Fluorescent albumin nanoparticles	130.3	0.353
Genexol-PM	27.7	0.109
Fluorescent micelles	27.6	0.151

Shown are the particle diameters of the fluorescent nanoparticles synthesized for transport studies in comparison to marketed paclitaxel formulations.

Table 3.2 Permeability across and uptake in BeWo cells

Formulation	Apparent permeability (cm/s)	% Uptake/mg protein
Fluorescent HSA nanoparticles	$1.98 \times 10^{-6} \pm 0.81 \times 10^{-6}$	0.099 ± 0.029
Fluorescent micelles	$59.5 \times 10^{-6} \pm 10.5 \times 10^{-6}$	0.057 ± 0.022
Abraxane	$4.95 \times 10^{-6} \pm 0.28 \times 10^{-6}$	–
Genexol-PM	$3.57 \times 10^{-6} \pm 2.14 \times 10^{-6}$	–

Apparent permeability and uptake of fluorescent HSA nanoparticles and micelles are shown (n=6 to 8 per group). For comparison, the permeability of paclitaxel in the formulations Abraxane and Genexol-PM across BeWo cells is also shown (n=6 or 7 per group).

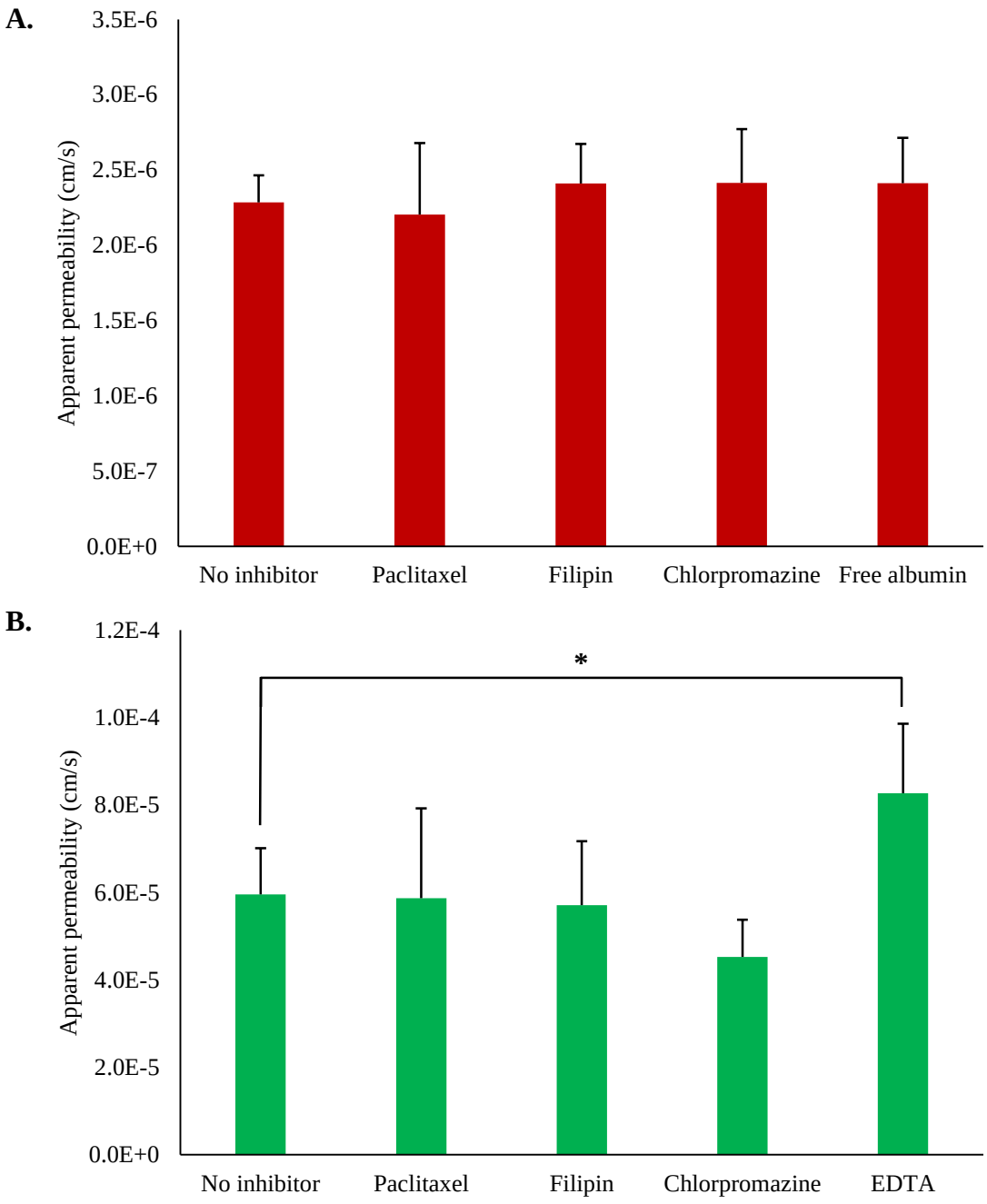

Figure 3.5 Effect of endocytosis inhibitors on permeability of fluorescent nanoparticles

(A) Effect of endocytosis inhibitors (paclitaxel, 20 µg/mL; filipin, 3 µg/mL; chlorpromazine, 10 µg/mL) on the permeability of albumin nanoparticles in BeWo cells, as well as a comparison to free fluorescent albumin, all at 2 hours (n=6 or 7). (B) Effect of endocytosis inhibitors (paclitaxel, filipin, and chlorpromazine) as well as EDTA (10 mM) on the permeability of fluorescent micelles across BeWo cells at 2 hours (n=7 or 8). Results were analyzed by ANOVA, followed by Tukey's HSD (*, $P < 0.001$). All error bars indicate standard deviation.

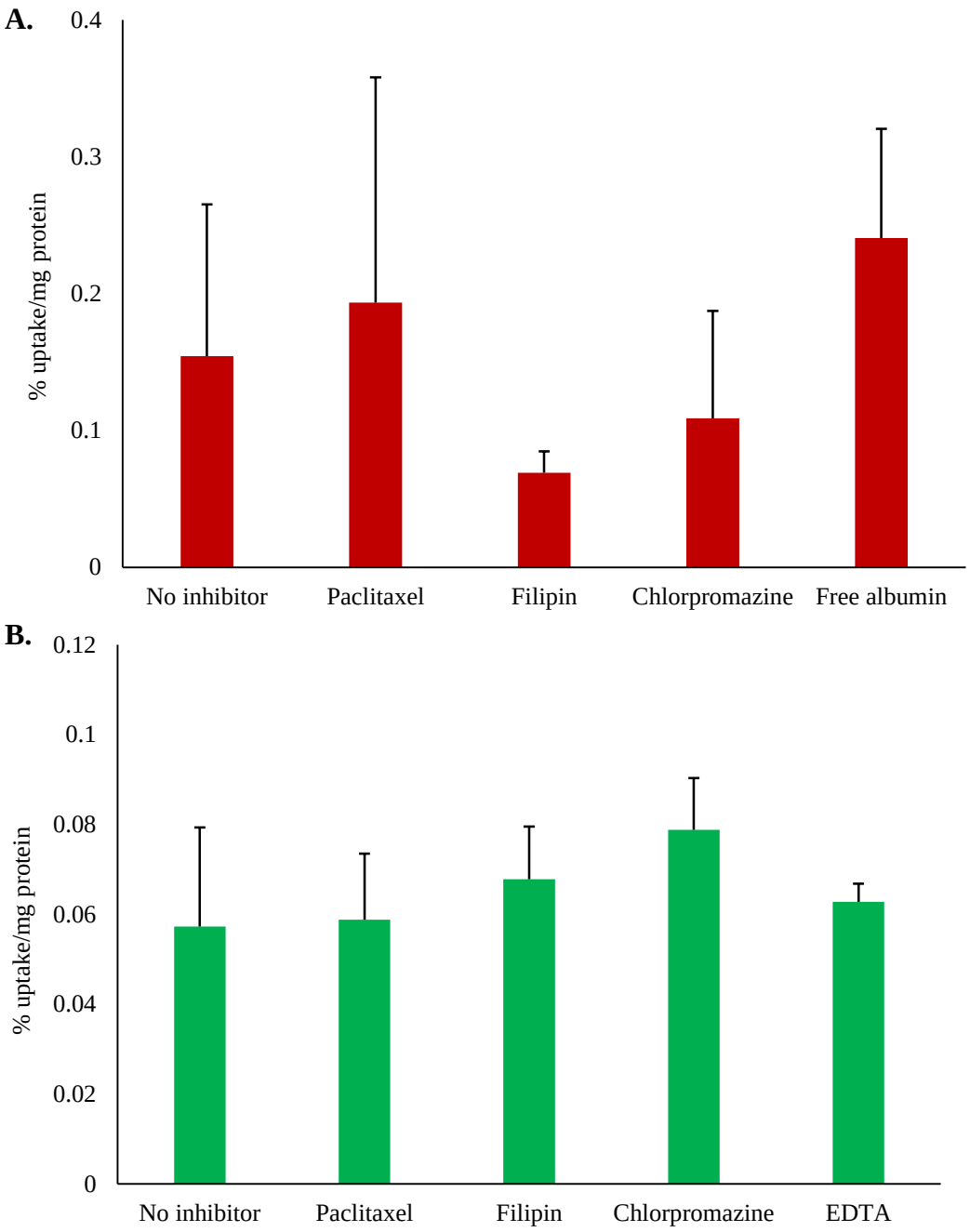

Figure 3.6 Effect of endocytosis inhibitors on fluorescent nanoparticle uptake

Uptake of fluorescent nanoparticles, calculated as the concentration present in cell lysate divided by the initial concentration and lysate protein concentration. (A) Effect of endocytosis inhibitors on fluorescent albumin nanoparticle uptake. (B) Effect of endocytosis inhibitors on fluorescent polymeric micelle uptake. Results were analyzed by ANOVA, followed by Tukey's HSD. No statistically significant differences observed.

CONCLUSION

Taken together, the information from these experiments points to similar behavior as was observed in placental perfusion studies. There were no formulation dependent differences in paclitaxel permeability between the three formulations, similar to the placental perfusion experiments. Cremophor-EL likely causes a reduction in the amount of paclitaxel that enters the trophoblast. It appears that Abraxane acts as the truest free drug formulation, due to its rapid disintegration. Upon administration with verapamil, paclitaxel permeability had the highest increase in the Abraxane group. Further, it appears that the permeability across BeWo cells of albumin, whether as free albumin or as a disintegrated nanoparticle, is very low. Genexol-PM was shown to cause a high paclitaxel accumulation in the tissue. We also showed that similarly sized fluorescent micelles can cross the placental trophoblast with high permeability. Whether this translates to increases in micelle concentration in fetal circulation or accumulation in the interstitial space or endothelium is still unknown.

Future studies would map out in multiple placental models how these different materials can interact with the placenta, and specifically if nanoparticle transport across BeWo cells correlates directly with increases in fetal concentration or simply interstitial accumulation. The role of fetal capillary endothelial cells in nanomaterial transport are still unknown, but it is possible that the fetal capillary endothelium prevents nanomaterial transport to fetal circulation.

Chapter 4. Conclusion and future directions

PROJECT SUMMARY

Paclitaxel is used in the treatment of breast cancer in pregnancy, in combination with other chemotherapeutic agents. Due to the limitations of the Taxol formulation of paclitaxel, as well as the potential pharmacokinetic benefits of nanoparticles, more companies have started formulating paclitaxel in a variety of nanoparticle delivery devices, some of which are already in clinical development or on the market. However, the impact of the incorporation of paclitaxel in nanoparticles on the transplacental transport of this drug is largely unknown. The work presented in this dissertation is meant to be the first step in understanding the effect of nanoparticle formulations on the transplacental transport of paclitaxel.

In Chapter 2, we examined the transplacental transport and placental uptake of paclitaxel in the *ex vivo* dually perfused human placental cotyledon. The advantages of this model are that it uses an intact human placenta, which helps account for the effect of the fetal endothelium, the placental stroma, and the trophoblast. The gross and microanatomy of the placenta is also preserved. As mentioned earlier, a disadvantage of this model is it is a human placenta delivered at term. Since it is known that placental anatomy and transporter expression change over the course of gestation, these models do not represent exactly the composition of the placenta before term. As an example, P-glycoprotein expression changes throughout pregnancy (14,67). However, the differences between formulations that can be seen in this model have translational value.

In Chapter 3, the BeWo cell model of the human placental trophoblast was used to examine further the mechanistic reasons behind the differences observed in Chapter 2. This model is highly reproducible and has been used extensively as a trophoblast model due to its functional efflux transporter expression (61). This model is limited in that the

effect of endothelium and placental stroma cannot be taken into account. However, using this model one can overcome interindividual variability that may mask true differences between formulations. Also, the specific effect of trophoblast cells on formulation uptake and transport can be examined in an isolated system, which is not possible in placental perfusions. This project used a combination of these two models to attempt to paint a more complete picture of the behavior of these materials in the placenta.

OVERALL IMPRESSIONS OF FINDINGS

Using the placental perfusion model, we were able to show that the fetal transfer rate of Taxol compared to Abraxane and Genexol-PM showed high variability which precluded the identification of significant differences between the groups. Maternal artery and reservoir concentrations of paclitaxel were significantly lower in perfusions of the nanoformulations than in Taxol, indicating that the excipients in different formulations play a large role in the interaction of these materials with the placenta. Taxol, which contains Cremophor-EL, most probably has an influence on the partitioning of paclitaxel between cell membranes and aqueous media, which may have resulted in higher media concentrations and lower tissue accumulation and transfer. In combination with placental lobule concentrations, it can be concluded that Genexol-PM causes a high degree of tissue accumulation of paclitaxel. Abraxane, which relies on the hydrophobic binding of paclitaxel to albumin, disintegrates upon dilution into aqueous media. The resulting albumin-bound paclitaxel likely acts as the truest free drug formulation of the three tested here.

Studies in BeWo cells with these paclitaxel formulations mirror the findings of placental perfusions (Figure 3.3). Taxol exhibited a marginal (not statistically significant) increase in permeability in the presence of verapamil, the P-gp inhibitor. This may also be due to the effect of Cremophor-EL on the partitioning of paclitaxel into the cell membrane,

because paclitaxel alone at 20 μg/mL had a more significant increase in permeability when administered with verapamil. Similar to Taxol was the behavior of Genexol-PM, which did not exhibit a high increase in permeability upon co-administration with verapamil. We showed that tissue uptake of Genexol-PM in placental perfusions was substantially higher than that of Taxol. This is an indication that, though the findings in BeWo cells are similar, the mechanism may have been due to Genexol-PM encapsulating paclitaxel and allowing it to cross the apical membrane of the trophoblast cells without being effluxed. Paclitaxel permeability increased sharply in the Abraxane group when verapamil was present, indicating that this formulation likely behaves most like free drug. This is expected since Abraxane disintegrates quickly upon dilution into media. The uptake in placental lobules between Taxol and Abraxane was very similar, with only a small and unsubstantial increase in uptake in the Abraxane group. True differences between these groups may potentially have been masked by either instrumental limitations or interindividual variability between perfusions. Due to these sources of error, accounting for complete mass balance is not easy to achieve. This method may not be sensitive enough for picking out minute differences in concentrations between groups.

Further studies were performed using fluorescent nanoparticles that had similar characteristics to the paclitaxel nanoformulations Abraxane and Genexol-PM. We were able to show in BeWo cells that the permeability of polymeric micelles is many times higher than that of albumin nanoparticles that have broken down to free albumin, even though the permeability of paclitaxel is the same. A reasonable conclusion from this would be that Genexol-PM may encapsulate paclitaxel and allow it to traverse the efflux barrier of the placental trophoblast, while albumin-bound paclitaxel may enter the trophoblast but dissociates quickly, subjecting it to P-gp efflux. Figure 4.1 shows our current understanding of the interaction of these materials with the placenta from the experiments shown here and from prior studies.

Abraxane:

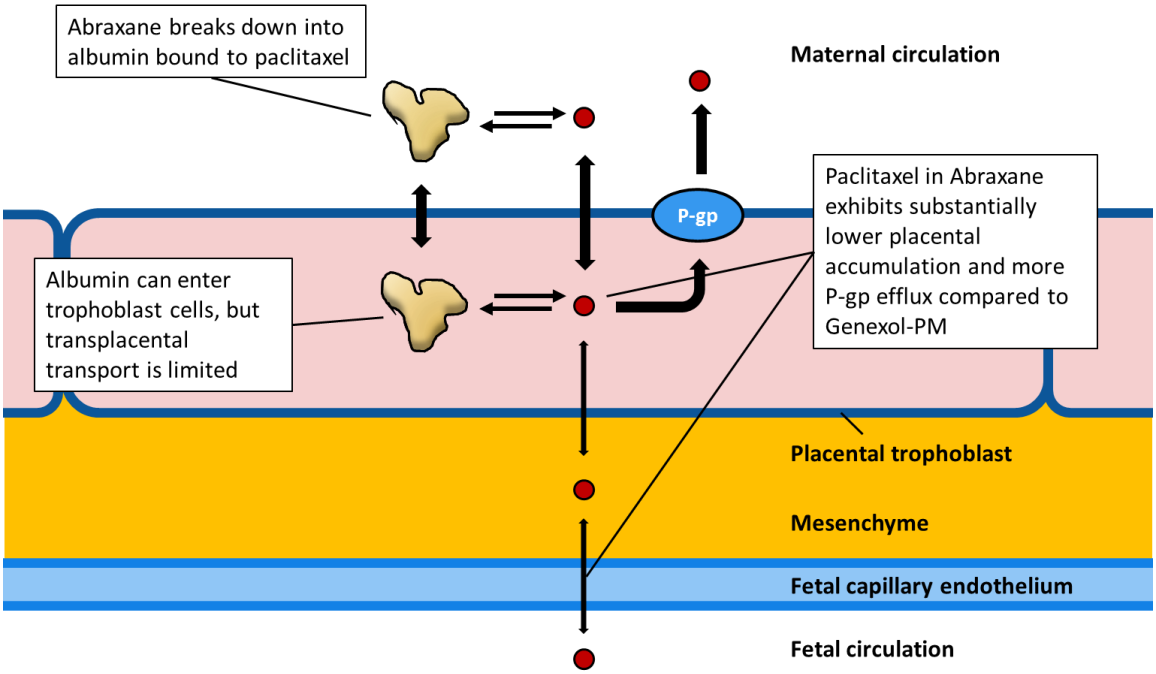

Genexol-PM:

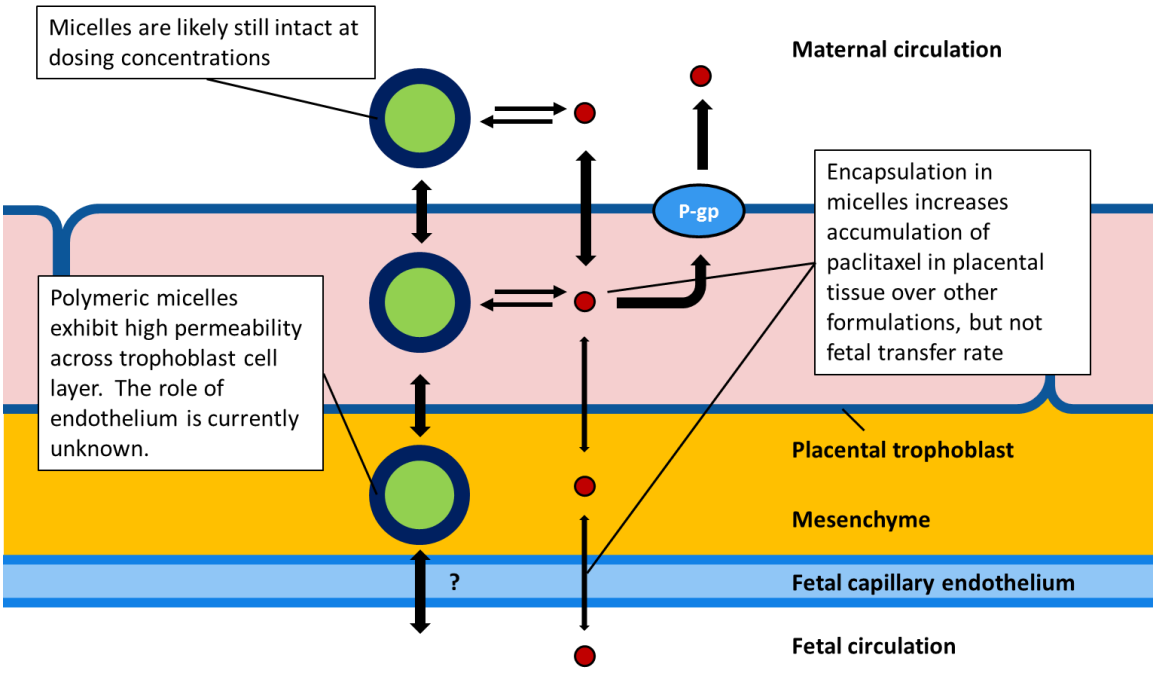

Figure 4.1 Interaction of Abraxane and Genexol-PM with the human placenta.

FUTURE STUDIES

There remain many questions to be answered regarding the interaction of Taxol, Abraxane, and Genexol-PM with placental tissue. Of primary concern is the degree to which these formulations can cross the placenta and accumulate in the placenta, and specifically the role that fetal capillary endothelium and placental stromal cells have on these nanoparticles. We have been able to show that some of the differences between the formulations are due to interactions with the trophoblast. The trophoblast is indeed considered the primary barrier for most xenobiotics, but the other cellular components of the placental trophoblast may play a role in nanoparticle transport. It is unknown whether fetal capillary endothelium allows for the transport of these nanoparticles into the fetal circulation, though previous placental perfusion studies with other types of nanoparticles have shown that this can occur.

Furthermore, the exact nature of the interaction of these materials with the placenta is unclear. It is known that albumin can enter trophoblast cells and many other cell types via specific endocytotic mechanisms that appear to be tissue specific. Based on prior literature and our studies, it is unlikely that this translates to a transcytosis in trophoblast cells, unlike what has been shown in endothelial cells that provide blood flow to tumors. Endocytosis mechanisms were probed in these studies and the permeability and uptake analyzed, but differences between groups were not substantial enough to say for certain that specific mechanisms were involved. It is possible that alternative methods of probing these mechanisms, including knock-down of proteins involved in specific pathways, may be able to show these differences. Removal of endocytosis capabilities by any method, however, will likely result in differences in cellular physiology and must be considered as a possible reason for any differences observed.

Another important consideration that should be examined in the future is the implication of increased uptake and transport of nanoparticles on the health of the placenta

and the health of the developing fetus. Increased placental accumulation and transplacental transfer of paclitaxel, a cytotoxic drug and inhibitor of mitosis, may be severely detrimental during pregnancy. We have shown that though there are some differences and high variability between the formulations in fetal transfer rate, the maternal concentrations and placental accumulation differ greatly. Future studies should examine the effects of drug accumulation on normal placental functions that are known, including endocrine regulation, nutrient transfer, and changes in transporter protein expression.

There are a number of other formulations of paclitaxel, and other drugs, that are entering clinical trials and, soon, the market. The effect of these nanoformulations on fetal exposure of drugs remains vastly understudied, and fetal exposure and placental accumulation of these compounds must therefore be carefully evaluated using appropriate *ex vivo*, *in vitro*, and *in vivo* models. Furthermore, an understanding of nanomaterial behavior, including drug release patterns and ability to traverse the placenta, should be taken into account when examining the effect of these formulations on transplacental drug transfer. Information on efflux/uptake of drugs and their nanoparticle excipients taken together can be of great benefit in generating hypotheses for how formulations under development may have a role in pregnancy, and also how to better design pharmaceuticals that are tailored towards use in pregnancy.

IMPLICATIONS FOR CLINICAL PRACTICE

This work was conducted in order to help us better understand the role of these nanoformulations in pregnancy. Though there is still a substantial amount that is currently unknown about their behavior, we have shown that the type of formulation has a profound effect on the disposition of the drug being delivered. It is very likely that these differences will translate into effects on fetal health and development, especially in the case of

paclitaxel. The data shown here, in combination with future studies, may help better formulate treatment strategies for breast cancer, including the gestational ages during which formulations may be administered and the type of formulations that should be avoided. There is a critical need to continue studying these effects, as more formulations—including nanoparticle formulations—of paclitaxel and a host of other drugs are entering the clinical trials and the market. It is also important to consider that bioequivalence of formulations in terms of pharmacokinetics may not necessarily translate into equivalent effects on the developing fetus or placenta. Ultimately, these differences should be taken into account by physicians and patients when prescribing treatments. We hope that the work presented here will promote a better understanding of the interaction of nanomaterials with the placenta. More importantly, we believe that this information is a step in the direction of safer pharmaceutical design and treatment strategies for breast cancer and other pregnancy related diseases.

Appendix

Appendix A. HPLC methods

APPENDIX A.1. CHROMATOGRAMS OF PACLITAXEL AND ANTIPYRINE IN PERFUSION MEDIUM SAMPLES

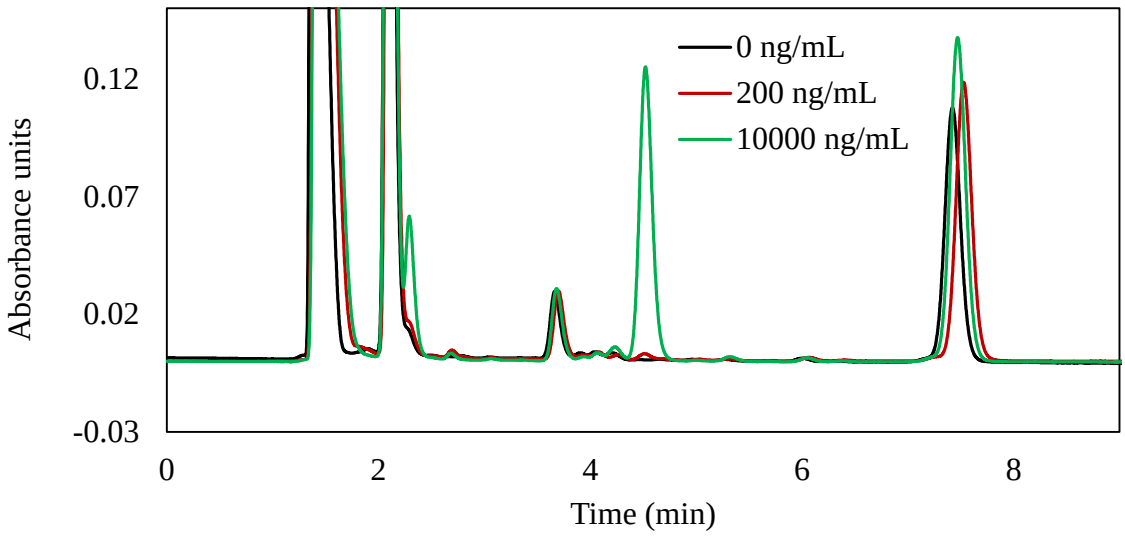

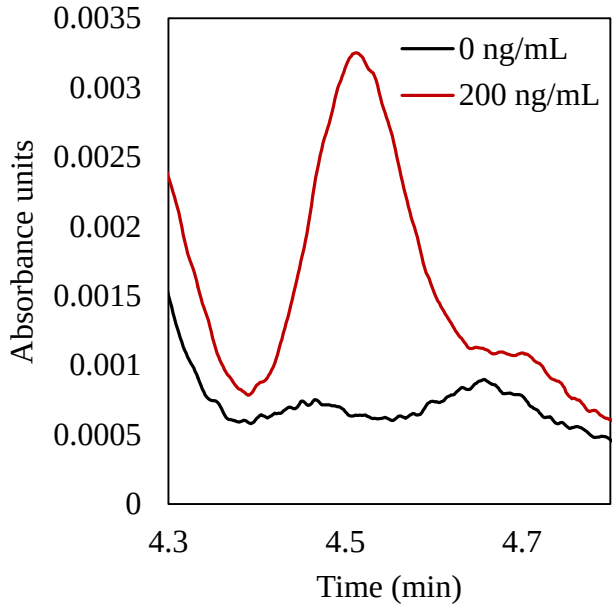

Paclitaxel detection by HPLC, using PDA detector (230 nm). Concentrations shown here are the lower limit of quantification (200 ng/mL) and half of the maximum concentration (10,000 ng/mL). Paclitaxel retention time is approximately 4.5 minutes, while celecoxib (internal standard) retention time is 7.2 minutes.

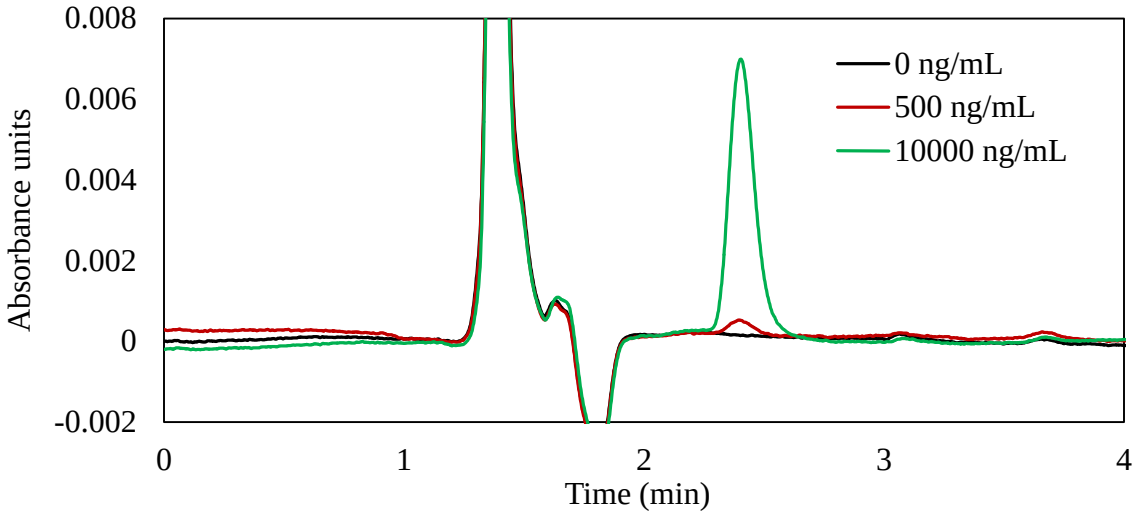

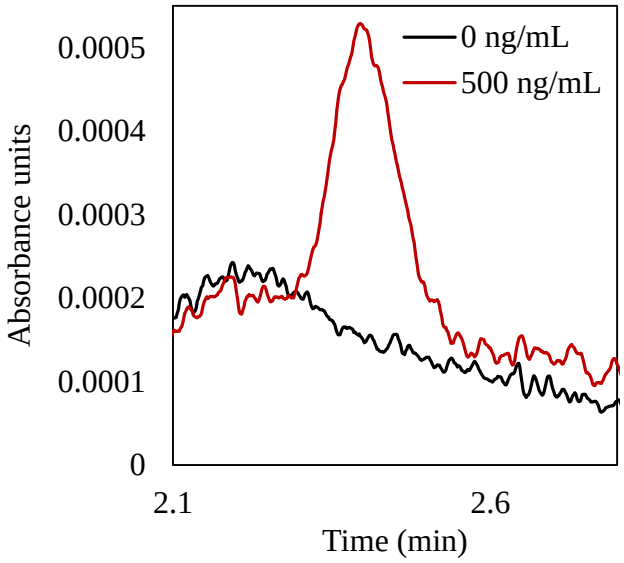

Antipyrine detection by HPLC using a PDA detector (243 nm). Concentrations shown here are the lower limit of quantification (500 ng/mL) and half of the maximum concentration (10000 ng/mL). Retention time of antipyrine is approximately 2.5 minutes.

APPENDIX A.2. STANDARD CURVES OF PACLITAXEL AND ANTIPYRINE IN PERFUSION MEDIUM

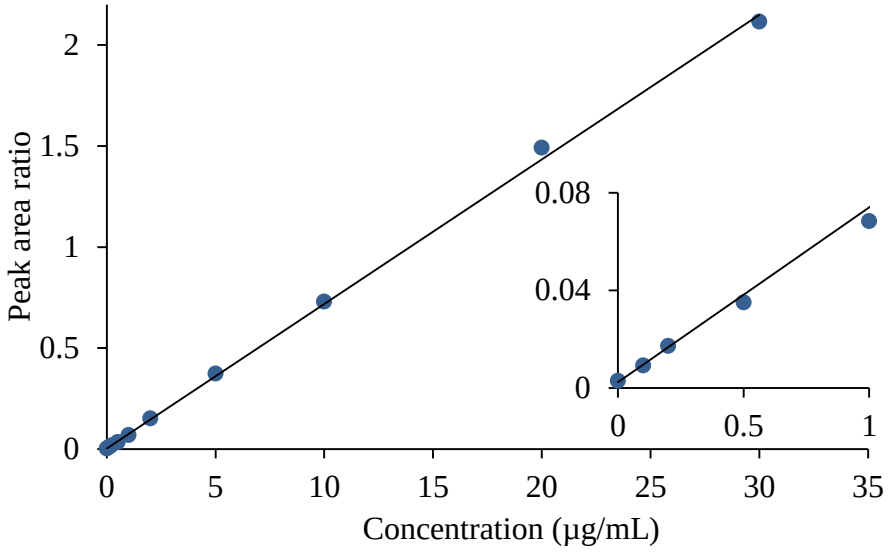

Standard curve of paclitaxel detection by HPLC, shown at 0-30,000 ng/mL and 0-1000 ng/mL (inset). *Peak area ratio* refers to the ratio of the peak area of paclitaxel to that of celecoxib (internal standard).

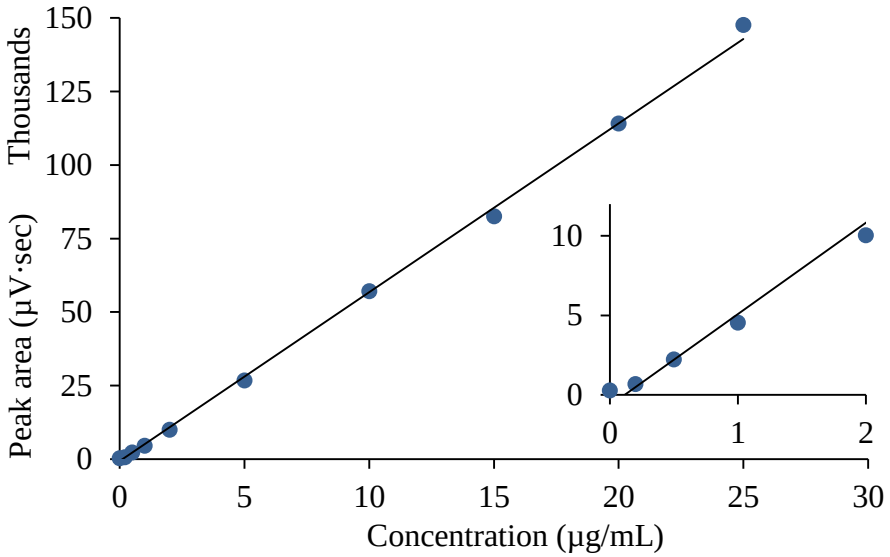

Standard curve of antipyrine detection by HPLC, shown at 0-25,000 ng/mL and 0-2000 ng/mL (inset).

APPENDIX A.3. LINEAR REGRESSION CHARACTERISTICS OF PACLITAXEL AND ANTIPYRINE DETECTION IN PERFUSION MEDIUM

	Slope	Y-intercept	R^2 value	LLOD (ng/mL)	LLOQ (ng/mL)
Paclitaxel	0.0716	0.0023	0.9961	100	200
Antipyrine	5741.0286	-668.9761	0.9989	200	500

LLOD, lower limit of detection.
LLOQ, lower limit of quantification

APPENDIX A.4. PRECISION, RECOVERY, AND ACCURACY OF PACLITAXEL AND ANTIPYRINE DETECTION IN PERFUSION MEDIUM

	Concentration (ng/mL)	Intra-day precision			Inter-day precision	Recovery	Accuracy
		Day 1	Day 2	Day 3			
Paclitaxel	200	7.2%	3.7%	8.9%	10.7%	58.9 ± 4.7%	101.1%
	10,000	2.9%	2.8%	1.5%	5.7%	60.5 ± 6.1%	102.3%
	20,000	2.9%	3.1%	2.8%	13.2%	65.6 ± 1.4%	105.7%
Antipyrine	500	8.9%	9.1%	7.3%	9.7%	95.1 ± 7.0%	98.2%
	10,000	1.9%	2.4%	4.1%	6.2%	103.5 ± 4.3%	100.1%
	20,000	5.1%	2.7%	0.6%	5.4%	99.5 ± 0.6%	97.9%

APPENDIX A.5. RECOVERY OF PACLITAXEL AND ANTIPYRINE IN PERFUSED MEDIA

	Spiked Concentration (ng/mL)	30 minute perfused medium		120 minute perfused medium	
		Precision	Recovery	Precision	Recovery
Paclitaxel	200	2.8%	45.3 ± 1.5%	7.1%	48.3 ± 2.6%
	10,000	3.2%	57.4 ± 2.0%	5.6%	69.2 ± 2.2%
	20,000	13.0%	54.2 ± 7.1%	5.5%	66.9 ± 2.5%
Antipyrine	500	12.4%	99.0 ± 5.4%	10.0%	104.5 ± 9.9%
	10,000	2.1%	97.6 ± 2.1%	3.2%	106.1 ± 3.4%
	20,000	1.6%	96.6 ± 1.6%	0.5%	99.9 ± 0.5%

APPENDIX A.6. HPLC SAMPLE STORAGE STABILITY

	Concentration (ng/mL)		
	Day 1	Day 8	Percent change
Paclitaxel	173	177	2.5%
	13,752	13,976	1.6%
	24,827	24,312	2.1%
Antipyrine	517	519	0.5%
	8780	8697	1.0%
	17,602	17,494	0.6%

APPENDIX A.7. STANDARD CURVE OF PACLITAXEL FROM TISSUE HOMOGENATE

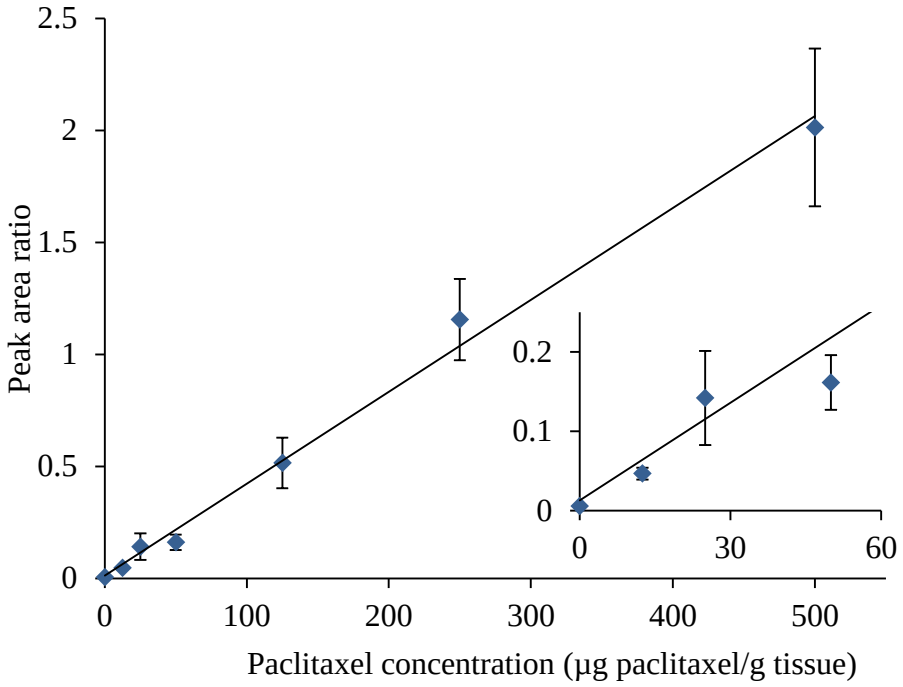

Paclitaxel concentrations determined by HPLC in tissue homogenate. Peak area ratio refers to the peak area of paclitaxel to that of celecoxib (internal standard). Error bars indicate standard deviation (n=3). Slope: 0.0041; Intercept: 0.00131; R^2: 0.9939.

Appendix B. Standard curves for transport studies

APPENDIX B.1. STANDARD CURVE OF PACLITAXEL IN CELL CULTURE MEDIA

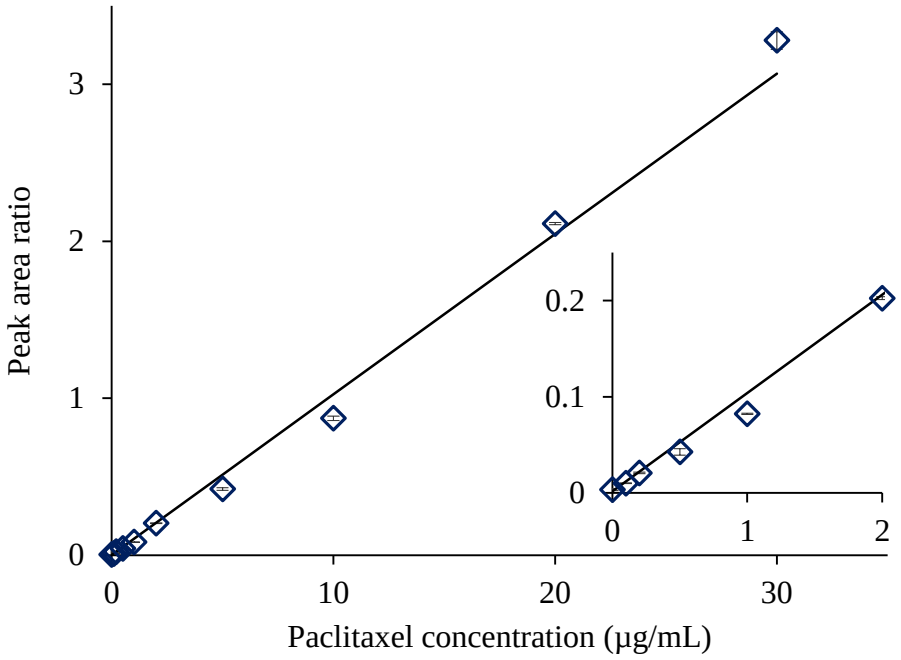

Paclitaxel concentrations determined by HPLC in cell culture media. Peak area ratio refers to the peak area of paclitaxel to that of celecoxib (internal standard). Error bars indicate standard deviation (n=3). Slope: 0.1022; Intercept: 0.0019; R^2: 0.9908.

APPENDIX B.2. STANDARD CURVES OF FLUORESCENT NANOPARTICLES

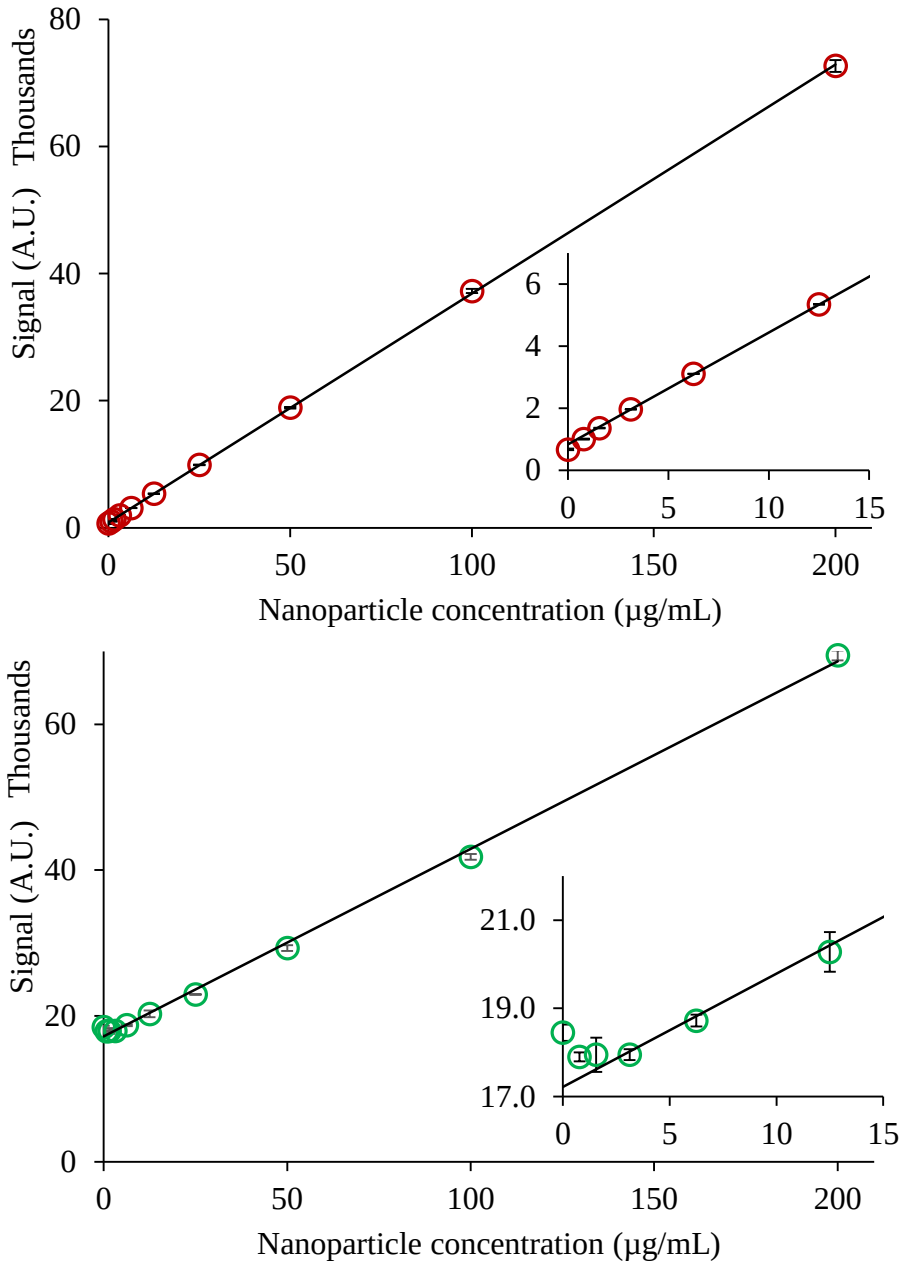

Standard curves of fluorescent albumin nanoparticles (top, $R^2 = 0.999$) and fluorescent polymeric micelles (bottom, $R^2 = 0.998$) in Hank's balanced salt solution, measured using a BioTek FLx800 fluorescence plate reader. Albumin nanoparticles were conjugated with fluorescein-NHS (λ_{ex}: 485/20, λ_{em}: 528/20). Polymeric micelles were conjugated with 7-methoxycoumarin-3-carbonyl azide (λ_{ex}: 330/40, λ_{em}: 400/30).

Appendix C. Placental perfusion antipyrine and paclitaxel concentrations, 240 minutes

Formulation	Perfusion	Antipyrine		Paclitaxel	
		Maternal artery	Fetal vein	Maternal artery	Fetal vein
Taxol	**1**	48.67%	48.39%	60.08%	11.83%
	2	39.75%	40.55%	45.44%	8.74%
	3	48.82%	51.77%	63.86%	19.50%
	4	45.47%	42.95%	40.27%	14.48%
Abraxane	**1**	48.53%	48.87%	33.51%	18.42%
	2	42.85%	56.64%	34.49%	11.26%
	3	50.43%	54.23%	44.00%	19.33%
	4	46.53%	41.99%	25.17%	14.88%
Genexol-PM	**1**	47.27%	46.57%	40.92%	19.95%
	2	41.29%	47.24%	35.31%	18.91%
	3	46.07%	47.55%	30.45%	18.10%
	4	52.80%	52.92%	26.74%	12.42%

Appendix D. Product characterization

APPENDIX D.1. HUMAN SERUM ALBUMIN CONJUGATION TO NHS-FLUORESCEIN

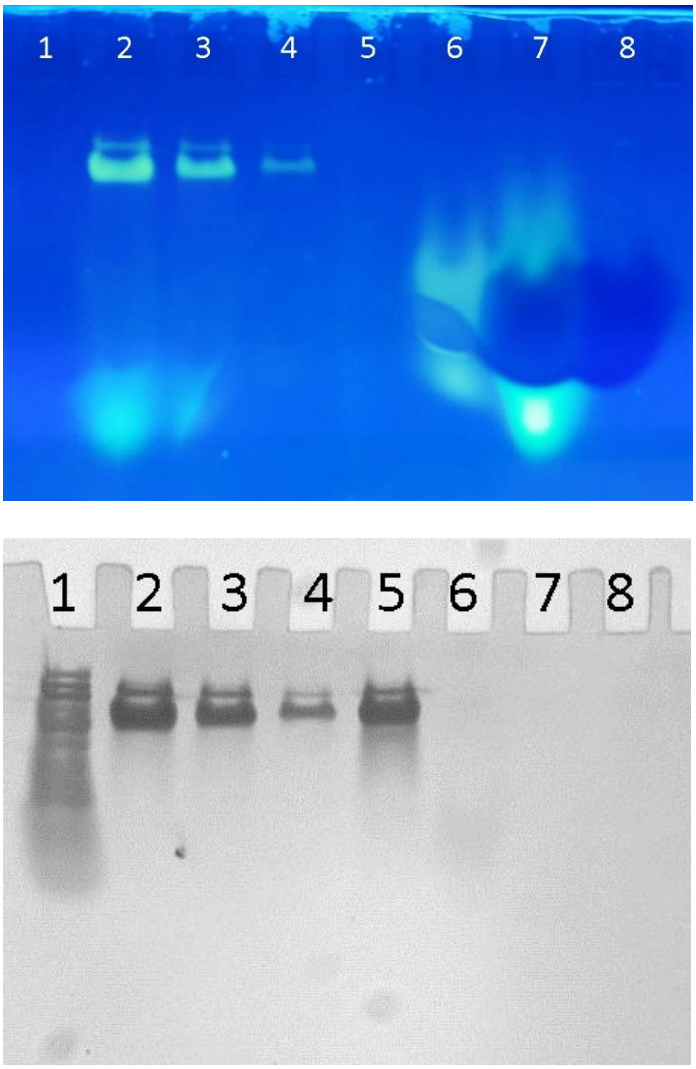

1. Protein ladder
2. HSA-fluorescein, crude (0.77 mg/mL)
3. HSA-fluorescein, crude (0.38 mg/mL)
4. HSA-fluorescein, crude (0.077 mg/mL)
5. HSA (1 mg/mL)
6. Free NHS-fluorescein
7. NHS-fluorescein + bromophenol blue
8. Bromophenol blue

Human serum albumin (HSA) conjugated to NHS-fluorescein. Separation of albumin from free fluorescein was performed by SDS-PAGE. UV illumination (top) shows the presence of free dye and HSA present in crude product (lanes 2-4). Free fluorescein appears to migrate slightly faster than bromophenol blue. Coomassie stain (bottom) shows fluorescein-bound HSA (lanes 2-4) with approximately the same molecular weight as unconjugated HSA (lane 5).

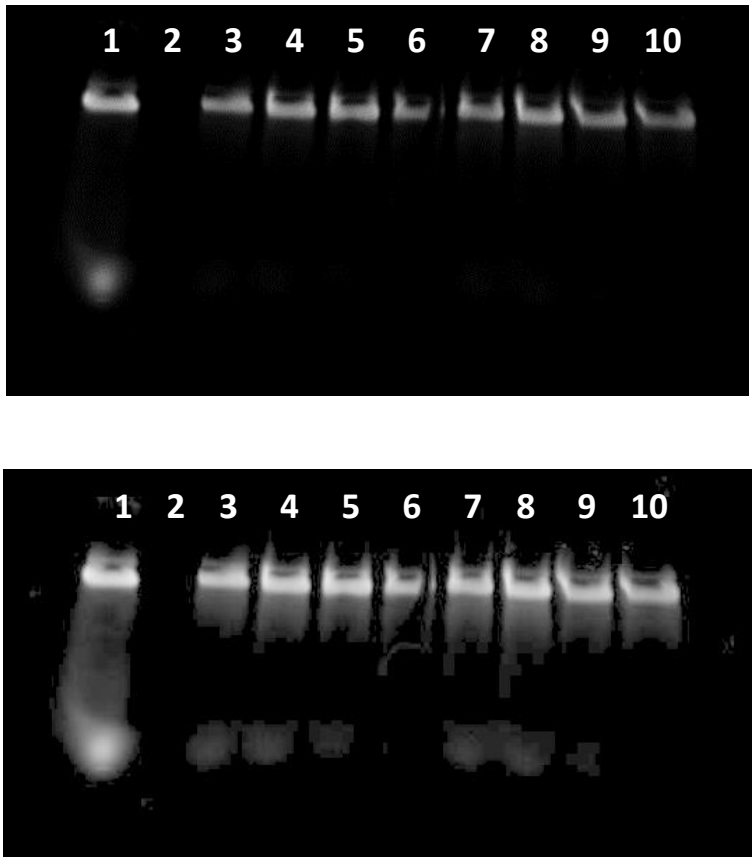

SDS-PAGE was used to determine the amount of free dye in HSA-fluorescein purified by size-exclusion chromatography (Sephadex G-25). Image was taken by an AlphaImager 2200 using UV illumination (λ_{em}: 537 nm). Lane 1 contains crude product, while lanes 3-10 contain purified product (top). The value of the image was altered to show the presence of trace amounts of free dye (bottom). Densitometry was used to calculate percent of fluorescent signal attributed to HSA-fluorescein:

Lane 1: 65%
Lanes 3, 4, 7, and 8: > 95%
Lanes 5, 6, 9, and 10: > 98%

APPENDIX D.2. PEG-PDLLA CONJUGATION TO 7-METHOXYCOUMARIN

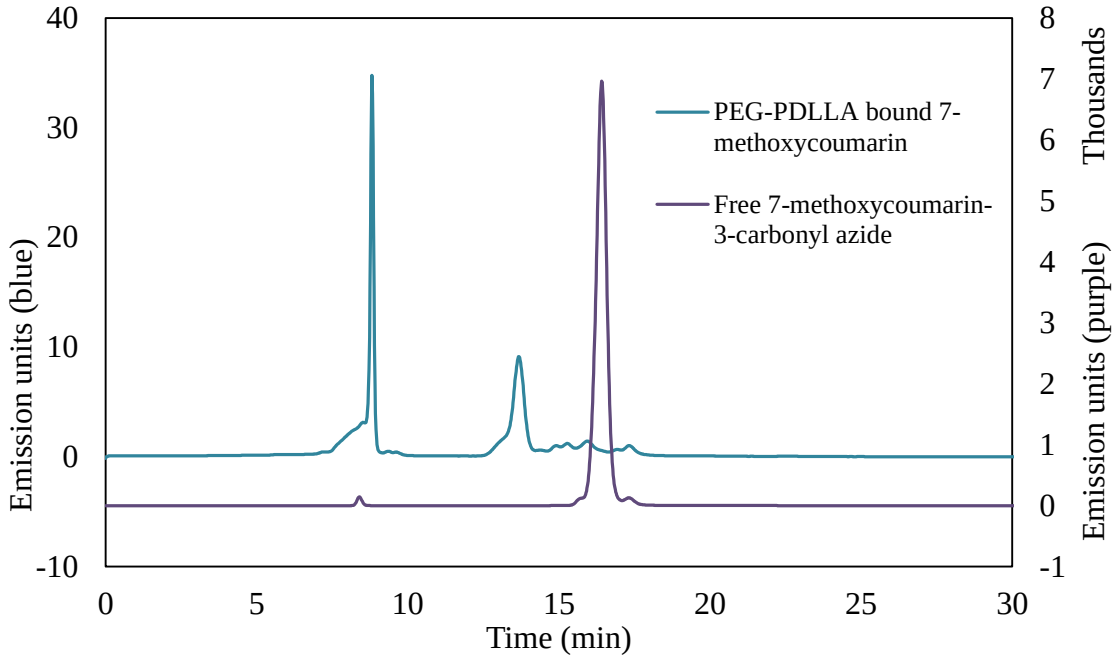

HPLC, equipped with a size exclusion column, was used to determine percent of conjugated dye in the purified product. Free 7-methoxycoumarin-3-carbonyl azide had a retention time of 16.4 minutes (right y-axis), which was less than 15% of the peak area of the purified product (left y-axis).

Column: Shodex OHpak SB-804HQ
Guard column: Shodex OHpak SB-G
Mobile phase: 50% acetonitrile, 50% deionized water
Flow rate: 0.7 mL/min
λ_{ex}: 330 nm
λ_{em}: 402 nm

APPENDIX D.3. SCREENING OF NANOPARTICLES

	HSA (% w/v)	Sonication time (min)	Particle size (nm)	PDI	Peak 1 (nm)	Peak 2 (nm)	Peak 3 (nm)
Abraxane	-	-	156.2	0.13	180.6	-	-
Blank HSA	5	1	2170.3	0.79	736.3	11.6	1.6
	5	2	3635.3	0.28	2501	270.4	7.4
	5	5	122	0.48	193.2	4.1	10.9
	5	8	84.1	0.6	179.2	7.452	-
Fluorescent HSA	5	8	262.1	0.264	336	-	-
	2.5	8	196.1[a]	0.465	265.1	-	-
	2.5	8	130.3[b]	0.353	205	-	-

HSA, human serum albumin; PDI, polydispersity index

a. Before filtration
b. After filtration (0.45 µm)

	Particle size (nm)	PDI
Genexol-PM	27.7 ± 0.5	0.109 ± 0.01
Blank micelles	20.8	0.186
Fluorescent micelles	22.4	0.082
Fluorescent micelles, lyophilized	27.6 ± 0.1	0.151 ± 0.02

Screening of fluorescent nanoparticles to be used in transport studies is shown. Albumin nanoparticles were prepared by sonication (top), where sonication time refers to total of all "on" pulses during sonication. Polymeric micelles (bottom) all exhibited only one peak by size distribution.

Appendix E. Toxicity of treatments

APPENDIX E.1. CYTOTOXICITY OF FORMULATIONS

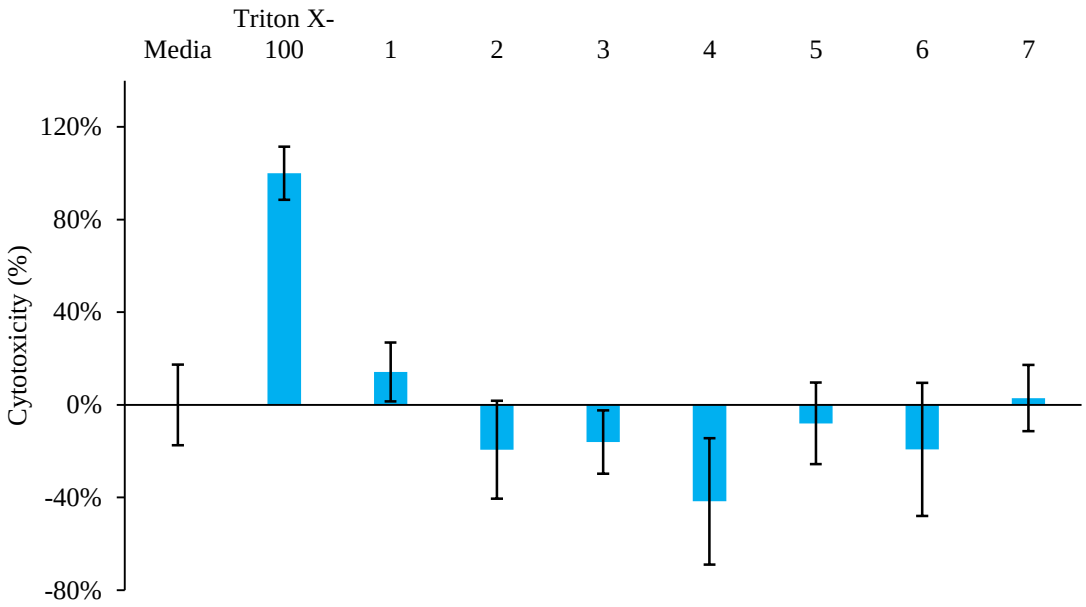

BeWo cells were treated with paclitaxel formulations, fluorescent nanoparticles, and Cremophor-EL for two hours. Triton X-100 is administered as a positive control (0.1% v/v). Toxicity was measured by LDH release using an LDH assay. Numbered labels are as follows:

1. Taxol (20 µg/mL paclitaxel)
2. Abraxane (20 µg/mL paclitaxel)
3. Genexol-PM (20 µg/mL paclitaxel)
4. Fluorescent micelles (200 µg/mL)
5. Fluorescent human serum albumin nanoparticles (200 µg/mL)
6. Paclitaxel in DMSO (20 µg/mL, final DMSO concentration was 0.1%)
7. Cremophor-EL (0.33 % v/v, equivalent to Taxol dose of 20 µg/mL paclitaxel)

APPENDIX E.2. CYTOTOXICITY OF INHIBITORS

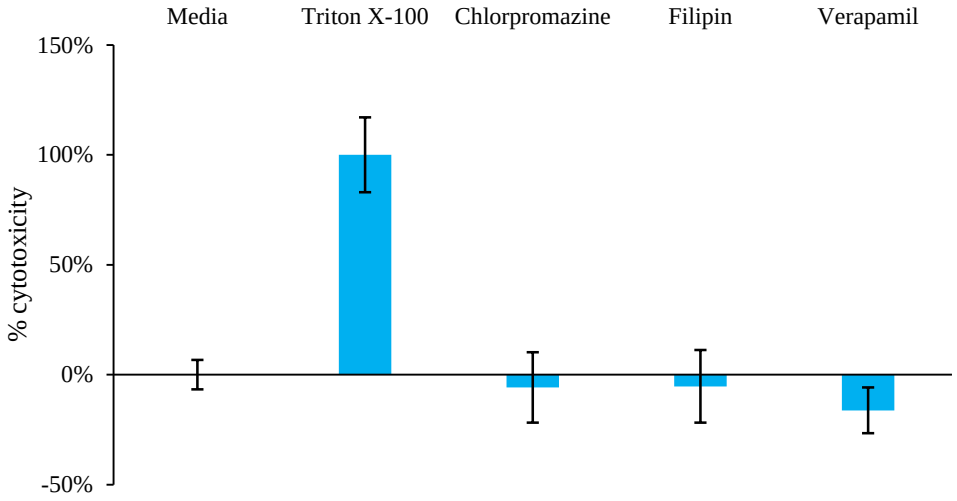

BeWo cells were treated with endocytosis inhibitors (filipin, 3 µg/mL; chlorpromazine, 10 µg/mL) and verapamil, a P-gp inhibitor (100 µM), for two hours. Toxicity was measured by LDH assay.

APPENDIX E.3. CYTOTOXICITY OF DMSO

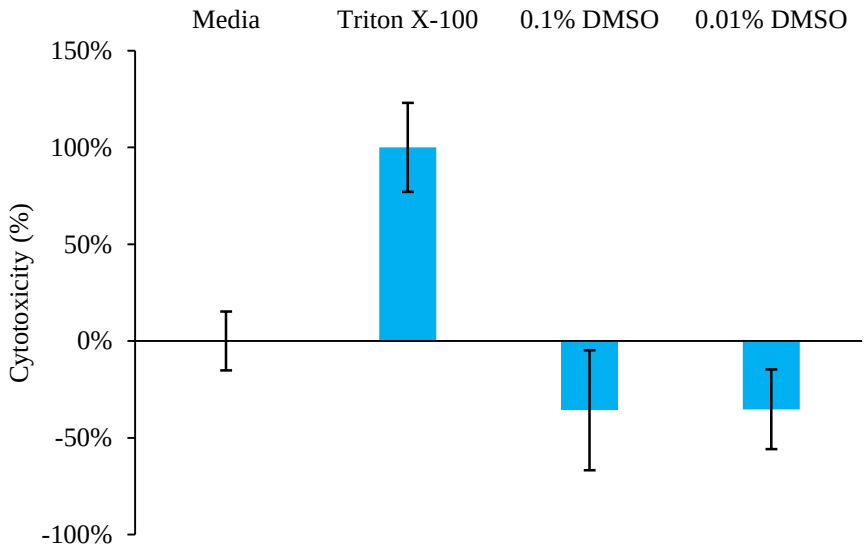

BeWo cells were treated with DMSO at two concentrations for 2 hours. DMSO was used as a carrier for filipin and paclitaxel. Toxicity was measured by LDH assay.

References

1. Salani R, Billingsley CC, Crafton SM. Cancer and pregnancy: An overview for obstetricians and gynecologists. *Am J Obstet Gynecol*. 2014 Jul;211(1):7–14.

2. Rimawi BH, Green V, Lindsay M. Fetal Implications of Diagnostic Radiation Exposure During Pregnancy : Recommendations. *Clin Obstet Gynecol*. 2016;59(2):412–8.

3. Kelly HL, Collichio FA, Dees EC. Concomitant pregnancy and breast cancer: Options for systemic therapy. *Breast Dis*. 2005;23:95–101.

4. Doyle S, Messiou C, Rutherford JM, Dineen RA. Cancer presenting during pregnancy: radiological perspectives. *Clin Radiol*. 2009;64(9):857–71.

5. Rovera F, Chiappa C, Coglitore A, Baratelli GM, Fachinetti A, Marelli M, et al. Management of breast cancer during pregnancy. *Int J Surg*. 2013 Dec;11(S1):S64–8.

6. Yang WT, Dryden MJ, Gwyn K, Whitman GJ, Theriault R. Imaging of breast cancer diagnosed and treated with chemotherapy during pregnancy. *Radiology*. 2006;239(1):52–60.

7. Breast Cancer [Internet]. National Comprehensive Cancer Network. 2016 [cited 2017 Feb 9]. https://www.nccn.org/professionals/physician_gls/pdf/breast.pdf

8. Peccatori, FA; Orecchia R. Cancer, pregnancy and fertility: ESMO Clinical Practice Guidelines for diagnosis , treatment and follow-up. *Ann Oncol*. 2013;21(May):1–11.

9. Amant F, Loibl S, Neven P, Van Calsteren K. Breast cancer in pregnancy. *Lancet*. 2012;379(9815):570–9.

10. Zagouri F, Sergentanis TN, Chrysikos D, Papadimitriou CA, Dimopoulos MA, Bartsch R. Trastuzumab administration during pregnancy: A systematic review and meta-analysis. *Breast Cancer Res Treat*. 2013;

11. Dekrem J, Van Calsteren K, Amant F. Effects of fetal exposure to maternal chemotherapy. *Pediatr Drugs*. 2013;15(5):329–34.

12. Cardonick E, Iacobucci A. Use of chemotherapy during human pregnancy. *Lancet Oncol*. 2004;5(5):283–91.

13. Zagouri F, Sergentanis TN, Chrysikos D, Dimitrakakis C, Tsigginou A, Zografos CG, et al. Taxanes for Breast Cancer during Pregnancy: A Systematic Review. *Clin Breast Cancer*. 2013 Feb;13(1):16–23.

14. Nanovskaya T, Nekhayeva I, Karunaratne N, Audus K, Hankins GD V, Ahmed MS. Role of P-glycoprotein in transplacental transfer of methadone. *Biochem Pharmacol*. 2005 Jun 15;69(12):1869–78.

15. Berveiller P, Vinot C, Mir O, Broutin S, Deroussent A, Seck A, et al. Comparative transplacental transfer of taxanes using the human perfused cotyledon placental model. *Am J Obstet Gynecol*. 2012 Dec;207(6):514.e1-514.e7.

16. McDaniel JR, Bhattacharyya J, Vargo KB, Hassouneh W, Hammer DA, Chilkoti A. Self-assembly of thermally responsive nanoparticles of a genetically encoded peptide polymer by drug conjugation. *Angew Chemie - Int Ed*. 2013;52(6):1683–7.

17. Nicolaou KC, Hale CRH, Nilewski C. A Total Synthesis Trilogy: Calicheamicin γ_1^I, Taxol®, and Brevetoxin A. *Chem Rec*. 2012 Aug 20;12(4):407–41.

18. Cooper GM. Microtubules. *The Cell: A Molecular Approach (2nd Ed)*.2000.

19. Weaver BA. How Taxol/paclitaxel kills cancer cells. *Mol Biol Cell*. 2014;25(18):2677–81.

20. Kim SCW, Kim DW, Shim YH, Bang JS, Oh HS, Kim SCW, et al. In vivo evaluation of polymeric micellar paclitaxel formulation: Toxicity and efficacy. *J Control Release*. 2001;72(1–3):191–202.

21. Gelderblom H, Verweij J, Nooter K, Sparreboom A. Cremophor EL: the drawbacks and advantages of vehicle selection for drug formulation. *Eur J Cancer*. 2001;37(13):1590–8.

22. Magidson V, He J, Ault JG, O'Connell CB, Yang N, Tikhonenko I, et al. Unattached kinetochores rather than intrakinetochore tension arrest mitosis in taxol-treated cells. *J Cell Biol*. 2016 Feb 1;212(3):307–19.

23. Spratlin J, Sawyer MB. Pharmacogenetics of paclitaxel metabolism. *Crit Rev Oncol Hematol*. 2007;61(3):222–9.

24. Fokina VM, Patrikeeva SL, Zharikova OL, Nanovskaya TN, Hankins GVD, Ahmed MS. Transplacental transfer and metabolism of buprenorphine in preterm human placenta. *Am J Perinatol*. 2011 Jan 6;28(1):25–32.

25. Bièche I, Narjoz C, Asselah T, Vacher S, Marcellin P, Lidereau R, et al. Reverse transcriptase-PCR quantification of mRNA levels from cytochrome (CYP) 1 , CYP2 and CYP3 families in 22 different human tissues. *Pharmacogenet Genomics*. 2007 Sep;17(9).

26. Nishimura M, Yaguti H, Yoshitsugu H, Naito S, Satoh T. Tissue distribution of mRNA expression of human cytochrome P450 isoforms assessed by high-sensitivity real-time reverse transcription PCR. *J Pharm Soc Japan*. 2003;123(5):369–75.

27. Pavek P, Smutny T. Nuclear receptors in regulation of biotransformation enzymes and drug transporters in the placental barrier. *Drug Metab Rev*. 2014;46(1):19–32.

28. Tian J, Stella VJ. Degradation of Paclitaxel and Related Compounds in Aqueous Solutions II: Nonepimerization Degradation Under Neutral to Basic pH Conditions. *J Pharm Sci*. 2008 Aug;97(8):3100–8.

29. Sofias AM, Dunne M, Storm G, Allen C. The battle of "nano" paclitaxel. *Adv Drug Deliv Rev*. 2017 Feb 28.

30. Untch M, Jackisch C, Schneeweiss A, Conrad B, Aktas B, Denkert C, et al. Nab-paclitaxel versus solvent-based paclitaxel in neoadjuvant chemotherapy for early breast cancer (GeparSepto—GBG 69): a randomised, phase 3 trial. *Lancet Oncol*. 2016 Mar;17(3):345–56.

31. Schettini F, Giuliano M, De Placido S, Arpino G. Nab-paclitaxel for the treatment of triple-negative breast cancer: Rationale, clinical data and future perspectives. *Cancer Treat Rev*. 2016 Nov;50:129–41.

32. Fu Q, Sun J, Zhang W, Sui X, Yan Z, He Z. Nanoparticle albumin-bound (NAB) technology is a promising method for anti-cancer drug delivery. *Recent Pat Anticancer Drug Discov*. 2009 Nov;4(3):262–72.

33. Werner ME, Cummings ND, Sethi M, Wang EC, Sukumar R, Moore DT, et al. Preclinical evaluation of genexol-pm, a nanoparticle formulation of paclitaxel, as a novel radiosensitizer for the treatment of non-small cell lung cancer. *Int J Radiat Oncol Biol Phys*. 2013 Jul 1;86(3):463–8.

34. Vergote I, Brize A, Lisyanskaya AS, Lichinitser M. Randomized phase III study comparing paclical-carboplatin with paclitaxel-carboplatin in patients with recurrent platinum-sensitive epithelial ovarian cancer. *J Clin Oncol*. 2015 May 20;33(15_suppl):5517.

35. Ye L, He J, Hu Z, Dong Q, Wang H, Fu F, et al. Antitumor effect and toxicity of Lipusu in rat ovarian cancer xenografts. *Food Chem Toxicol*. 2013 Feb;52:200–6.

36. Koudelka S, Turánek J. Liposomal paclitaxel formulations. *J Control Release*. 2012 Nov 10;163(3):322–34.

37. Jain MM, Gupte SU, Patil SG, Pathak AB, Deshmukh CD, Bhatt N, et al. Paclitaxel injection concentrate for nanodispersion versus nab-paclitaxel in women with metastatic breast cancer: a multicenter, randomized, comparative phase II/III study. *Breast Cancer Res Treat*. 2016 Feb 3;156(1):125–34.

38. Nehate C, Jain S, Saneja A, Khare V, Alam N, Dubey RD, et al. Paclitaxel formulations: challenges and novel delivery options. *Curr Drug Deliv*. 2014;11(6):666–86.

39. Yassine F, Salibi E, Gali-Muhtasib H. Overview of the Formulations and Analogs in the Taxanes' Story. *Curr Med Chem*. 2016;23(40):4540–58.

40. Hubbell JA, Chilkoti A. Carbon Nanomaterials for Drug Delivery. *Science*. 2012;337(2012):303–5.

41. Albanese A, Tang PS, Chan WCW. [Review] The Effect of Nanoparticle Size, Shape, and Surface Chemistry on Biological Systems. *Annu Rev Biomed Eng*. 2012 Aug 15;14(1):1–16.

42. Ali S, Rytting E. Influences of Nanomaterials on the Barrier Function of Epithelial Cells. *Adv Exp Med Biol*. 2014;811:45–54.

43. Boonsongrit Y, Mitrejev A, Mueller B. Chitosan drug binding by ionic interaction. *Eur J Pharm Biopharm*. 2006 Apr;62(3):267–74.

44. Ernsting MJ, Murakami M, Roy A, Li S-D. Factors controlling the pharmacokinetics, biodistribution and intratumoral penetration of nanoparticles. *J Control Release*. 2013 Dec 28;172(3):782–94.

45. Kobayashi H, Watanabe R, Choyke PL. Improving conventional enhanced permeability and retention (EPR) effects; What is the appropriate target? *Theranostics*. 2014;4(1):81–9.

46. Grafmueller S, Manser P, Diener L, Diener P-A, Maeder-Althaus X, Maurizi L, et al. Bidirectional Transfer Study of Polystyrene Nanoparticles across the Placental Barrier in an ex Vivo Human Placental Perfusion Model. *Environ Health Perspect*. 2015 May 8;123(12):1280–6.

47. Ali H, Kalashnikova I, White MA, Sherman M, Rytting E. Preparation, characterization, and transport of dexamethasone-loaded polymeric nanoparticles across a human placental in vitro model. *Int J Pharm*. 2013 Sep 15;454(1):149–57.

48. Albekairi NA, Al-Enazy S, Ali S, Rytting E. Transport of digoxin-loaded polymeric nanoparticles across BeWo cells, an in vitro model of human placental trophoblast. *Ther Deliv*. 2015 Dec;6(12):1325–34.

49. Doherty GJ, McMahon HT. Mechanisms of Endocytosis. *Annu Rev Biochem*. 2009 Jun;78(1):857–902.

50. Desai NP, Tao C, Yang A, Louie L, Yao Z, Soon-Shiong P, et al. Protein stabilized pharmacologically active agents, methods for the preparation thereof and methods for the use thereof. US Patent 6,749,868.

51. Oncologic Drugs Advisory Committee Meeting briefing [Internet]. 2012 [cited 2017 Jan 1]. https://www.fda.gov/ohrms/dockets/ac/06/briefing/2006-4235B2-01-01AbraxisBioscience-background.pdf

52. Lambot N. Evidence for a Clathrin-Mediated Recycling of Albumin in Human Term Placenta. *Biol Reprod*. 2006;75(1):90–7.

53. Nekhayeva IA, Nanovskaya TN, Pentel PR, Keyler DE, Hankins GD V, Ahmed MS. Effects of nicotine-specific antibodies, Nic311 and Nic-IgG, on the transfer of nicotine across the human placenta. *Biochem Pharmacol*. 2005 Nov 25;70(11):1664–72.

54. Kim SC, Kim DW, Shim YH, Bang JS, Oh HS, Wan Kim S, et al. In vivo evaluation of polymeric micellar paclitaxel formulation: toxicity and efficacy. *J Control Release*. 2001 May 14;72(1–3):191–202.

55. Next-Generation Cancer Therapeutics [Internet]. [cited 2017 Apr 18]. https://www.sec.gov/Archives/edgar/data/850261/000119312513363203/d595928dex993.htm

56. Wick P, Malek A, Manser P, Meili D, Maeder-Althaus X, Diener L, et al. Barrier capacity of human placenta for nanosized materials. *Environ Health Perspect*. 2010;118(3):432–6.

57. Burton GJ, Jauniaux E. What is the placenta? *Am J Obstet Gynecol*. 2015;213(4):S6.e1-S6.e4.

58. Prouillac C, Lecoeur S. The Role of the Placenta in Fetal Exposure to Xenobiotics: Importance of Membrane Transporters and Human Models for Transfer Studies. *Drug Metab Dispos*. 2010 Oct 1;38(10):1623–35.

59. Hemauer SJ, Nanovskaya TN, Abdel-Rahman SZ, Patrikeeva SL, Hankins GD V, Ahmed MS. Modulation of human placental P-glycoprotein expression and activity by MDR1 gene polymorphisms. *Biochem Pharmacol*. 2010;79(6):921–5.

60. Ceckova-Novotna M, Pavek P, Staud F. P-glycoprotein in the placenta: Expression, localization, regulation and function. *Reprod Toxicol*. 2006;22(3):400–10.

61. Utoguchi N, Chandorkar GA, Avery M, Audus KL. Functional expression of P-glycoprotein in primary cultures of human cytotrophoblasts and BeWo cells. *Reprod Toxicol*. 2000;14(3):217–24.

62. Bhattacharyya J, Bellucci JJ, Weitzhandler I, McDaniel JR, Spasojevic I, Li X, et al. A paclitaxel-loaded recombinant polypeptide nanoparticle outperforms Abraxane in multiple murine cancer models. *Nat Commun*. 2015 Aug 4;6:7939.

63. Boschetti-de-Fierro A, Voigt M, Storr M, Krause B, Krediet RT. MCO Membranes: Enhanced Selectivity in High-Flux Class. *Sci Rep*. 2016 Nov 16;5(1):18448.

64. Mcpartland TJ, Patil RA, Malone MF, Roberts SC. Liquid-liquid extraction for

recovery of paclitaxel from plant cell culture: Solvent evaluation and use of extractants for partitioning and selectivity. *Biotechnol Prog*. 2012;28(4):990–7.

65. Vasantha J, Kannan G, Goud T, Palani T, Vanitha R, Anitha R, et al. Pharmacokinetic evaluation of Paclitaxel in South Indian cancer patients: a prospective study. *J Young Pharm*. 2011;3(4):322–8.

66. Syme MR, Paxton JW, Keelan JA. Drug Transfer and Metabolism by the Human Placenta. *Clin Pharmacokinet*. 2004;43(8):487–514.

67. Gil S, Saura R, Forestier F, Farinotti R. P-glycoprotein expression of the human placenta during pregnancy. *Placenta*. 2005 Feb;26(2–3):268–70.

68. Akour AA, Kennedy MJ, Gerk P. Receptor-Mediated Endocytosis across Human Placenta: Emphasis on Megalin. *Mol Pharm*. 2013 Apr 1;10(4):1269–78.

69. Hemauer SJ, Patrikeeva SL, Nanovskaya TN, Hankins GD V, Ahmed MS. Role of human placental apical membrane transporters in the efflux of glyburide, rosiglitazone, and metformin. *Am J Obstet Gynecol*. 2010;202(4):383.e1-383.e7.

70. Al-Enazy S, Ali S, Albekairi N, El-Tawil M, Rytting E. Placental control of drug delivery. *Adv Drug Deliv Rev*. 2016 Aug 12.

71. Soininen SK, Repo JK, Karttunen V, Auriola S, Vähäkangas KH, Ruponen M. Human placental cell and tissue uptake of doxorubicin and its liposomal formulations. *Toxicol Lett*. 2015 Dec 3;239(2):108–14.

72. Majeed SR, Vasudevan L, Chen C-Y, Luo Y, Torres JA, Evans TM, et al. Clathrin light chains are required for the gyrating-clathrin recycling pathway and thereby promote cell migration. *Nat Commun*. 2014 May 23;5:3891.

73. Smith-Jackson K, Hentschke MR, Poli-de-Figueiredo CE, Pinheiro da Costa BE, Kurlak LO, Broughton Pipkin F, et al. Placental expression of eNOS, iNOS and the major protein components of caveolae in women with pre-eclampsia. *Placenta*. 2015 May;36(5):607–10.

74. Akour AA, Gerk P, Kennedy MJ. Megalin expression in human term and preterm placental villous tissues: Effect of gestational age and sample processing and storage time. *J Pharmacol Toxicol Methods*. 2015 Jan;71:147–54.

75. Rashid-Doubell F, Tannetta D, Redman CWG, Sargent IL, Boyd CAR, Linton EA. Caveolin-1 and Lipid Rafts in Confluent BeWo Trophoblasts: Evidence for Rock-1 Association with Caveolin-1. *Placenta*. 2007 Feb;28(2–3):139–51.

76. Desai N, Trieu V, Damascelli B, Soon-Shiong P. SPARC Expression Correlates with Tumor Response to Albumin-Bound Paclitaxel in Head and Neck Cancer Patients. *Transl Oncol*. 2009;2(2):59–64.

77. Cartwright L, Poulsen MS, Nielsen HM, Pojana G, Knudsen LE, Saunders M, et al. In vitro placental model optimization for nanoparticle transport studies. *Int J Nanomedicine*. 2012;7:497–510.

78. Luo L, Tam J, Maysinger D, Eisenberg A. Cellular internalization of poly(ethylene oxide)-b-poly(epsilon-caprolactone) diblock copolymer micelles. *Bioconjug Chem*. 13(6):1259–65.

79. Hemauer SJ, Patrikeeva SL, Nanovskaya TN, Hankins GDV, Ahmed MS. Opiates inhibit paclitaxel uptake by P-glycoprotein in preparations of human placental inside-out vesicles. *Biochem Pharmacol*. 2009 Nov 1;78(9):1272–8.

80. Vähäkangas K, Myllynen P. Drug transporters in the human blood-placental barrier. *Br J Pharmacol*. 2009 Oct;158(3):665–78.

81. Bode CJ, Jin H, Rytting E, Silverstein PS, Young AM, Audus KL. In vitro models for studying trophoblast transcellular transport. *Methods Mol Med*. 2006;122:225–39.

82. Vidricaire G, Tremblay MJ. A clathrin, caveolae, and dynamin-independent endocytic pathway requiring free membrane cholesterol drives HIV-1 internalization and infection in polarized trophoblastic cells. *J Mol Biol*. 2007 May 18;368(5):1267–83.

83. Delorme-Axford E, Sadovsky Y, Coyne CB. Lipid raft- and SRC family kinase-dependent entry of coxsackievirus B into human placental trophoblasts. *J Virol*. 2013 Aug 1;87(15):8569–81.

84. Kumari S, Mg S, Mayor S. Endocytosis unplugged: multiple ways to enter the cell. *Cell Res*. 2010 Mar 2;20(3):256–75.

85. Rejman J, Bragonzi A, Conese M. Role of clathrin- and caveolae-mediated endocytosis in gene transfer mediated by lipo- and polyplexes. *Mol Ther*. 2005 Sep;12(3):468–74.

86. Herd H, Daum N, Jones AT, Huwer H, Ghandehari H, Lehr C-M. Nanoparticle Geometry and Surface Orientation Influence Mode of Cellular Uptake. *ACS Nano*. 2013 Mar 26;7(3):1961–73.

87. Blanchard E, Belouzard S, Goueslain L, Wakita T, Dubuisson J, Wychowski C, et al. Hepatitis C virus entry depends on clathrin-mediated endocytosis. *J Virol*. 2006 Jul;80(14):6964–72.

88. Deli MA. Potential use of tight junction modulators to reversibly open membranous barriers and improve drug delivery. *Biochim Biophys Acta - Biomembr*. 2009;1788(4):892–910.

Vita

Shariq Ali was born in London, England, on July 1st, 1989. He was born to Drs. Nawab and Afshan Ali. Shariq attended Little Rock Central High School and the University of Arkansas at Little Rock. He earned a Bachelor of Science degree at the University of Arkansas at Little Rock. Shariq has co-authored three peer-reviewed original research articles, one review, and two book chapters.

Permanent address: 7109 N Holiday Dr., Galveston, TX 77550

This dissertation was typed by Shariq Ali.